Fish condition as an indicator of stock status: Insights from condition index in a food-limiting environment

Ines Haberle[1], Lav Bavčević[2], Tin Klanjscek[1,*]

March 2023

[1] Ruđer Bošković Institute, Bijenička cesta 54, 10002 Zagreb, Croatia

[2] Department of Ecology, Agriculture and Aquaculture, University of Zadar, M. Pavlinovića 1, 23000 Zadar, Croatia

[*] Corresponding author: tin@irb.hr (Tin Klanjscek)

This is the accepted version of the following article:
Haberle, I., Bavčević, L., & Klanjscek, T. (2023). Fish condition as an indicator of stock status: Insights from condition index in a food-limiting environment. *Fish and Fisheries, 00*, 1-15 which has been published in final form at `https://doi.org/10.1111/faf.12744`.

This article may be used for noncommercial purposes in accordance with the Wiley Self-Archiving Policy [`http://www.wileyauthors.com/selfarchiving`].

Abstract

Individual performance defines population dynamics. Condition index – a ratio of weight and some function of length – has been louded as an indicator of individual performance and recommended as a tool in fisheries management and conservation. However, insufficient understanding of the correlation between individual-level processes and population-level responses hinders its adoption. To this end, we use composite modelling to link individual's condition, expressed through the condition index, to population-level status. We start by modelling ontogeny of European pilchard (*Sardina pilchardus*, Clupeidae) as a function of food and constant temperature using Dynamic Energy Budget theory. We then provide a framework to simultaneously track the individual- and population-level statistics by incorporating the DEB model into an individual-based model. Lastly, we explore the effects of fishing pressure on the statistics in two constant and food-limited environmental carrying capacity scenarios. Results show that, regardless of the species' environmental carrying capacity, individual condition index will increase with fishing mortality, i.e. with reduction of stock size. Same patterns are observed for gilthead seabream (*Sparus aurata*, Sparidae), a significantly different species. Condition index can, therefore, in food-limited populations, be used to (i) estimate population size relative to carrying capacity, and (ii) distinguish overfished from underfished populations. Our findings promote a practical way to operationally incorporate the condition index into fisheries management and marine conservation, thus providing additional use for the commonly collected biometric data. Some real-world applications, however, may require additional research to account for other variables such as fluctuating environmental conditions and individual variability.

Keywords

Dynamic Energy Budget, fisheries management, fishing mortality, individual-based model, *Sardina pilchardus*, *Sparus aurata*

Contents

1 Introduction

2 Material and Methods

2.1 Model species

2.2 Dynamic Energy Budget (DEB) model

2.3 Individual-based model (IBM)

2.4 Fishing mortality

2.5 Simulations

2.6 Outputs and analysis

3 Results

3.1 Effects of fishing

3.2 Impact of environmental carrying capacity

4 Discussion

5 Conclusions

Author Contributions

Acknowledgments

Conflict of Interest Statement

Data Availability Statement

References

Supplementary Information

1 Introduction

Effective decision-making in fisheries management and marine conservation relies on data- and model-driven scientific advice. Traditionally, the advice is derived from analytical stock assessments that rely on time series of catch-per-unit-effort measures, abundance indices, and age structure data (Quinn & Deriso, 1999; Tesfaye & Getahun, 2021). Due to the effort required for their collection, such data is however missing for more than 80% of the world fisheries (Costello et al., 2012; Mu et al., 2021). Length and weight data, on the other hand, are commonly collected even in the local small-scale fisheries (Dennis et al., 2015; Mackinson et al., 2017). Although very simple, these biometric measurements hold much more information than they are usually credited for. Length correlates with many attributes of the organism. It is crucial in monitoring evolutionary and ecological consequences of size-selective harvesting (Fenberg & Roy, 2008; Neumann & Allen, 2007; Rodríguez-Castañeda et al., 2022; Uusi-Heikkilä, 2020), and can be used as a proxy of metabolic rates and maintenance metabolism to help identify initiation of reproduction (Chen et al., 2022). Weight, as it correlates with the size of the ovary and the number of ova, has been identified as one of the most cost-efficient indicator of fecundity (Ahti et al., 2021). Combined into a ratio, length and weight result in a new metric - condition index.

Condition index is routinely used when investigating individual ontogeny because it adds value to the information provided by the two biometric measurements alone. For example, the index has been identified as a good indicator of energy status and physical condition of the fish, and related to their performance including growth, reproduction, and swimming ability (Bavčević et al., 2020; Martinez et al., 2003; Schloesser & Fabrizio, 2017). Furthermore, it can be used to identify physiological state of individuals and, consequently, assess their survival and future reproductive success (Mu et al., 2021).

Individual performance defines population dynamics, hence information within the condition index should, in principle, contain information on the status of the population. Such information could then be used in stock assessment and the associated decision-making. Many authors therefore generally recommend the use of condition index in fisheries management, but do not provide practical means of doing so (Anderson & Neumann, 1996; Blackwell et al., 2000; Bolin et al., 2021; Lloret et al., 2012; Stevenson &

Woods, 2006). The true potential of condition index for fisheries management cannot be realized because understanding of correlations between individual-level processes and population-level responses is lacking. Hence, managers cannot link the condition index to the status of the population, and are hesitant to use it in decision-making. Identifying the links between these two levels of biological organization would therefore arguably greatly foster the process of integrating condition index into standard management practice.

We use mechanistic individual-based modelling approach to explore these correlations. Individual-based models (IBMs) are intrinsically built to simultaneously track individuals and their population, and are therefore, convenient to investigate their correlation (DeAngelis & Mooij, 2005; Grimm et al., 2016; Grimm & Railsback, 2005). Recently, integration of IBMs with general theories capturing variability in individual ontogeny as a function of environmental variables greatly improved model predictions (Martin et al., 2012; Stillman et al., 2015), and allowed for generalization of the model outcomes.

Our (composite) IBM accounts for feedbacks between the environment, the individual, and the population. Dynamic Energy Budget (DEB) model is used to link the environment to individual-level outcomes, while a NetLogo-based IBM accounts for population-level effects. This enables simultaneous tracking of individual- and population-level statistics, and allows exploration of the effects of fishing mortality and environmental carrying capacity, on both.

Results show that, regardless of the environmental carrying capacity, individual condition index will increase as fishing mortality increases, and population size decreases. We discuss that condition index can be used as a good indicator of population size relative to its food-limited carrying capacity, and can help distinguishing underfishing from imminent stock collapse. Given constrains of our model, we suggest a careful integration of condition index considerations into regular fisheries management and conservation practices. This would also promote exploitation of commonly collected biometric data - lenght and weight - to create meaningful information that can support scientific-based decision-making.

2 Material and Methods

We integrated Dynamic Energy Budget (DEB) model into an individual-based model (IBM), a practice proven to efficiently translate individuals' performance to population dynamics (Beaudouin et al., 2015; Goedegebuure et al., 2018; Grimm et al., 2016; Martin et al., 2013; Maury & Poggiale, 2013). The composite model was used to simultaneously track both physiological traits and population dynamics of the fish. We simulated two food availability levels representing high and low environmental carrying capacity scenarios. For each scenario, we investigated effects of fishing pressure ranging from zero, representing natural non-exploited population, to overfishing. As a primary model species we choose extensively fished small pelagic European pilchard (*Sardina pilchardus*, Clupeidae). To validate the approach and verify robustness of the results, the whole procedure was repeated for a biologically and ecologically contrasting fish species, a demersal predator gilthead seabream (*Sparus aurata*, Sparidae). Methods and Results of the main text focus on European pilchard; the details for gilthead seabream are in the Supplement S1.

2.1 Model species

European pilchard occupies open waters of the Mediterranean Sea and the Eastern Atlantic along the coast from Great Britain to Senegal (GBIF Secretariat, 2021). It exhibits typical schooling behaviour, moving between depths of 10 m at night and up to 100 m at day (Froese & Pauly, 2022). Sardines forage on a wide range of prey size spectrum, dominated by mesozooplanktonic copepodes, and express both filter (non-selective) and particulate (selective) feeding driven by the availability of large prey (Nikolioudakis et al., 2012). The maximal adult size ranges from 17.5 to 27 cm, with average life span of 8 years (Froese & Pauly, 2022; Silva et al., 2008). Juveniles reach maturity during first two years, becoming batch spawners at around 50% of their maximal size (Froese & Pauly, 2022; Véron et al., 2020). Breeding period is determined by the geographical area, lasting for three to five consecutive months during one season (Whitehead, 1985). European pilchard is economically important in the European Union and North Africa, where it is exclusively wild fished, with production of around 1.5 million $^{\text{tonnes}}/_{\text{year}}$ since 2018 (FAO, 2022).

2.2 Dynamic Energy Budget (DEB) model

The individual level statistics were simulated using the DEB theory principles. This theory mechanistically describes energy fluxes into and within the organism throughout ontogeny, and as a function of environmental conditions (Figure 1; Kooijman 2010; Sousa et al. 2008). The theory is based on mathematical equations describing physiological processes of assimilation, growth, maintenance, maturation and reproduction. Below, we describe the main considerations of the DEB modelling approach. Further details can be found in the relevant DEB literature (Jusup et al., 2017; Kooijman, 2010, 2014; Marques et al., 2018; Sousa et al., 2008).

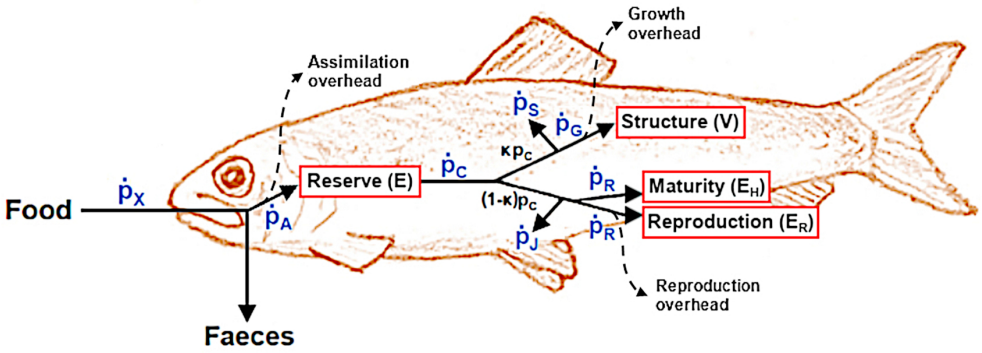

Figure 1: Schematic representation of a Dynamic Energy Budget (DEB) model with associated state variables (boxes) and energy fluxes (arrows). State variables: energy reserve (E), structure (V), maturity (E_H), reproduction buffer (E_R). Energy fluxes: $\dot{p}_X$ - ingestion, $\dot{p}_A$ - assimilation, $\dot{p}_C$ - mobilization, $\dot{p}_S$ - somatic maintenance, $\dot{p}_G$ - growth, $\dot{p}_J$ - maturity maintenance, $\dot{p}_R$ - maturation before/reproduction after reaching sexual maturation. A fixed fraction of energy, $\kappa\dot{p}_C$, is mobilized into somatic branch (somatic maintenance and growth), while the remaining energy, $(1-\kappa)\dot{p}_C$, is directed into the reproductive branch (maturity maintenance, and maturation or reproduction). Overhead fluxes (dashed arrows) account for energy losses associated with assimilation, growth, and reproduction.

State variables Within DEB, the organism is divided into four conceptual compartments described by abstract state variables - structure, reserve, maturity, and reproduction buffer. Structural compartment relates to the size of the individual, and requires energy for growth and metabolic work (maintenance). The reserve compartment stores assimilated energy, and provides energy for metabolic processes. Maturity is associated with increase in general complexity of the organism, and enables modelling of life-stage transitions (birth, metamorphosis, and sexual maturation). Energy investment into ma-

turity ceases at sexual maturation, but some energy is dissipated for maintenance of the acquired maturity level throughout the life of the individual. Reproduction buffer corresponds to the energy stored for production of reproductive tissue and gametes once sexual maturation is reached. Structure, reserve, and reproduction buffer contribute to the weight of the organism, maturity does not.

DEB models typically assume that material composition of each compartment stays constant, but the composition differs between compartments. Overall composition of the organism is, therefore, variable: as the ratio of energy stored in compartments vary, so does the overall composition of the organism. While the composition of energy reserves may be biased towards more lipids when reserves are high, the total weight of the fish is only marginally affected, and therefore we assume a constant energy reserve composition. In cases where the composition changes have the potential to affect results, an additional long-term storage compartment can be considered (Martin et al., 2017).

Energy fluxes The dynamics of energy within each compartment are determined by energy fluxes (Table 1). Ingestion of energy through food, and its storage into the reserve, are respectively described by ingestion ($\dot{p}_X$) and assimilation ($\dot{p}_A$). A part of ingested energy is returned into the environment as faeces, with the rest being assimilated into reserve (Figure 1). Because we are only interested into the energy effectively used by the organism, we account for the assimilated energy only, i.e. energy that can further be mobilized from the reserve by the catabolic flux ($\dot{p}_C$).

Energy is mobilized into two distinct branches: (i) a somatic branch for maintenance of somatic processes ($\dot{p}_S$) and growth ($\dot{p}_G$), and (ii) reproductive branch for maintaining maturity ($\dot{p}_J$) and investment into maturation before sexual maturity, or reproduction afterwards ($\dot{p}_R$). Reabsorption of energy from the reproduction buffer can occur in extreme cases of starvation, when mobilization from the energy reserve is not sufficient to pay somatic and maturity maintenance costs (Kooijman, 2010). Assimilation, growth, and reproduction are characterized by costs of metabolic transformations causing energy losses, addressed by specific fractions of energy going to the related overhead fluxes.

Table 1: General equations of the Dynamic Energy Budget (DEB) model describing energy fluxes, dynamics of state variables, and translation into observable metrics. Parameters are defined in Table 2.

DEB energy flux

Assimilation†	$\dot{p}_A = f\{\dot{p}_{Am}\} s_M L^2$	(1)
Mobilization‡	$\dot{p}_C = [E] \cdot \frac{\dot{v} s_M [E_G] V^{2/3} + \dot{p}_S}{\kappa [E] + [E_G]}$	(2)
Somatic maintenance	$\dot{p}_S = [\dot{p}_M] V$	(3)
Maturity maintenance	$\dot{p}_J = \dot{k}_J E_H$	(4)
Growth	$\dot{p}_G = \kappa \dot{p}_C - \dot{p}_S$	(5)
Maturation/Reproduction	$\dot{p}_R = (1-\kappa)\dot{p}_C - \dot{p}_J$	(6)

† Assimilation starts at birth, i.e. when $E_H \geq E_H^b$; it is equal to 0 before birth.

‡ $[E]$ stands for energy density, E/V.

Dynamics of the DEB state variables

Reserve energy	$\frac{d}{dt}E = \dot{p}_A - \dot{p}_C$	(7)
Structural body volume	$\frac{d}{dt}V = \frac{\dot{p}_G}{[E_G]}$	(8)
Energy invested into maturation	$\frac{d}{dt}E_H = \dot{p}_R$ while $E_H < E_H^p$	(9)
Energy invested into reproduction	$\frac{d}{dt}E_R = \dot{p}_R$ when $E_H = E_H^p$	(10)

Calculation of biological metrics

Physical length	$L_w = \frac{V^{1/3}}{\delta_M}$	(11)
Weight	$W_w = \mathrm{w}\big(d_V V + \frac{\omega_E}{\mu_E}(E + E_R)\big)$	(12)
Fertility§	$N_{eggs} = \kappa_R \frac{E_R}{E_0}$	(13)

§ Initial energy reserve of an egg, E_0, is calculated based on the energy reserve of the mother, i.e. following the rules of maternal effect (see footnote ¶ in Table 2).

Parameters Given the DEB model, energy dynamics are determined by species-specific parameters (listed in Table 2). The parameter values are obtained through parameterisation based on empirical data (Lika et al., 2011), a process performed for more than 900 fish species to date (AmP, 2023). Auxiliary parameters relate the abstract DEB quantities to the observable metrics such as physical length, weight, and fertility. Parameter values for European pilchard were taken from the corresponding entry in the Add-my-Pet collection (Nunes et al., 2019).

Fish undergo metamorphosis, implying that specific physiological adaptations occur throughout their early development. Within DEB, this is addressed by introduction of metabolic acceleration between birth and metamorphosis (Kooijman et al., 2011; Kooijman, 2014), incorporated through acceleration factor s_M. The value of the parameter s_M

directly affects energy assimilation and mobilization (Table 1); it equals unity at birth, increases until metamorphosis, and stays constant afterwards (see footnote § in Table 2).

Table 2: Dynamic Energy Budget (DEB) model parameters for European pilchard, taken from the Add-my-Pet collection entry (Nunes et al., 2019). The dots above the letters denote rates, while square and curly brackets relate to volume- and surface-specific quantities, respectively.

Primary DEB parameters	**Symbol**	**Value**	**Unit**
Maximal surface-specific searching rate†	$\{\dot{F}_m\}$	6.5	$^{l}/_{d\ cm^2}$
Maximum surface-specific assimilation rate	$\{\dot{p}_{Am}\}$	396.002	$^{J}/_{d\ cm^2}$
Fraction of food energy fixed in reserve†	κ_X	0.80	–
Allocation fraction to soma	κ	0.945	–
Fraction of reproduction energy fixed in eggs	κ_R	0.95	–
Energy conductance	$\dot{v}$	0.0172	$^{cm}/_{d}$
Volume-specific somatic maintenance rate	$[\dot{p}_M]$	396.195	$^{J}/_{d\ cm^3}$
Volume-specific costs of structure	$[E_G]$	5197	$^{J}/_{cm^3}$
Maturity maintenance rate coefficient	$\dot{k}_J$	0.002	$/_{d}$
Maturation threshold for birth	E_H^b	0.0112	J
Maturation threshold for metamorphosis	E_H^j	0.3478	J
Maturation threshold for sexual maturation	E_H^p	3013	J

†Used to calculate half-saturation constant K_X

Auxiliary DEB parameters	**Symbol**	**Value**	**Unit**
Half-saturation constant‡	K_X	235	$^{J}/_{l}$
Shape coefficient	δ_M	0.1152	-
Specific structure density	d_V	0.2	$^{g}/_{cm^3}$
Mass-energy-weight couplers	ω_E	23.9	$^{g}/_{mol}$
	μ_E	550000	$^{J}/_{mol}$
Wet/dry weight coefficient	w	5	-
Acceleration factor§	s_M	$min(\frac{L}{L_b}, \frac{L_j}{L_b})$	-
Inital energy reserve of an egg ¶	E_0	$\frac{E_{0max}-E_{0min}}{[E_m]-[E_{pmin}]}\big([E]-[E_{pmin}]\big)+E_{0min}$	J

‡ Calculated as $\frac{\{\dot{p}_{Am}\}s_M}{\kappa_X\{\dot{F}_m\}}$, and rounded to the nearest 5.

§ Acceleration factor changes with size up to metamorphosis, and is calculated as a ratio of current size L to the size at birth L_b, $\frac{L}{L_b}$. It stays equal to $\frac{L_j}{L_b}$ after metamorphosis, where L_j is size at metamorphosis.

¶ Determined according to maternal effect, i.e. depends on the actual energy density of the mother $[E]$. $[E_m]$ and $[E_{pmin}]$ are the maximal and minimal energy densities of a fertile mother, producing viable eggs with respectively maximal, E_{0max}, and minimal, E_{0min}, initial energy reserve.

2.3 Individual-based model (IBM)

Our IBM was built in the freely available NetLogo 6.2.1 software, specialized to facilitate construction of IBMs (Wilensky, 1999). The IBM simulates interdependent dynamics of each individual separately in a common environment over a chosen period of time (decades) quantized into much smaller time-steps (1 day in our simulations). For each time-step, the IBM first calculates whether the individual survives using the *Survival* module. Based on the food availability provided by the *Food update* module, *DEB* module then calculates energy acquisition for each survivor, energy allocation to growth, maturation (in juveniles) and reproduction (in adults); it also executes starvation strategy of re-absorbing energy from reproduction buffer to pay maintenance costs, if energy mobilisation from reserve is not sufficient. *Maturation* module transfers all matured juveniles into adults. *Spawning* module, called up during the spawning season, allocates the reproduction buffer of each individual into eggs, according to calculated inital energy reserves. Energy dynamics of the eggs is also tracked within the *DEB* module, and their hatching is governed by the *Hatching* module. *Aging* module tracks the age of each individual. Individual physical and physiological attributes, and the emerging population dynamics, are tracked throughout the simulation. A detailed description of the composite DEB-IBM and all included submodels is given in the Supplement S2, following the standard 'Overview, Design concepts, and Details' (ODD) protocol for describing IBMs (Grimm et al., 2006, 2010, 2020).

Environment Environment was defined by two factors: temperature, and food availability. In our model, temperature was a fixed parameter, kept constant at 20°C in all simulations. Food in our model is the sole determinant of the environmental carrying capacity for fish that is equal to the steady state of non-fished stock. We simulated high and low food levels, corresponding to high and low carrying capacity scenarios. In both scenarios, total available food for the day was provided at the beginning of each time-step as a fixed amount, X. The low food availability, representing a low environmental carrying capacity, was set such that daily available food concentration corresponded to the half-saturation constant of European pilchard rounded down to the nearest 10, i.e. $X = 230\ \mathrm{J/l} \approx K_X$. The higher food availability of $X = 11500\ \mathrm{J/l}$, set at approximately 50 times the half-saturation constant, represented a high environmental carrying capacity.

We assumed food availability is equal for all, i.e. all individuals perceive the same amount of food leading to the same communal functional response, f_{comm}, determining eventual energy assimilation. To calculate f_{comm} we followed a general definition by Martin et al. (2017): functional response can be interpreted as the ratio of the food consumed in one day to the maximum food that could be consumed in a day,

$$f_{comm} = \frac{\dot{p}_A}{\dot{p}_{Amax}}. \tag{14}$$

Assuming that complete available prey can potentially be consumed by the population, the global food assimilation in one day ($\dot{p}_A$) equals the assimilation of the total daily available food

$$\dot{p}_A = \frac{\kappa_X X W_V}{\Delta t} \tag{15}$$

where X is the food concentration, W_V is the volume of the system, κ_X is the food energy fixation efficiency, and Δt is the model time-step (1 day). The maximum food that could in principle be consumed in a day by the population ($\dot{p}_{Amax}$) is determined as a sum of individual maximal assimilation ($\dot{p}_{Amax_i}$, i indicating individual) of its N individuals according to the their size L_i,

$$\dot{p}_{Amax} = \sum_{i=1}^{N} \dot{p}_{Amax_i} = \sum_{i=1}^{N} \left\{\dot{p}_{Am}\right\} s_{M_i} L_i^2. \tag{16}$$

The f_{comm} is then the ratio of Eq. 15 to Eq. 16:

$$f_{comm} = min\left(\frac{\dot{p}_A}{\dot{p}_{Amax}}, 1\right) = min\left(\frac{\kappa_X X W_V}{\Delta t \sum_{i=1}^{N} \left\{\dot{p}_{Am}\right\} s_{M_i} L_i^2}, 1\right). \tag{17}$$

Note that when food is abundant, the numerator in Eq. 17 is equal or larger than denominator, and f_{comm} will be 1. If the food is scarce, $\dot{p}_A$ is lower than the $\dot{p}_{Amax}$, and the f_{comm} will be lower than 1.

To test the robustness of our results we also considered alternative food availability approach, a chemostat type food dynamics as described in De Roos et al. (1990). There, we also used the communal functional response as described above, except the daily food availability X was a result of the chemostat dynamics, rather than a fixed amount. While we discuss the implications of the alternative in the Discussion, details and results of this

approach are included in the Supplement S3.

Individuals The incorporation of individuals into the DEB-IBM framework followed the practice of previously published DEB-IBMs (Beaudouin et al., 2015; Goedegebuure et al., 2018; Martin et al., 2013). Individuals contribute towards population dynamics through survival, growth, and recruitment (determined by hatching, maturation, and spawning), each calculated within designated submodel (Supplement S2.7). These are driven by the individual energy dynamics, captured with the DEB submodel. The assimilation of each individual is a crucial step that affects its interaction with both environment, and other individuals through intraspecific competition.

The individual assimilation, $\dot{p}_{A_i}$, was calculated in a standard DEB fashion, however driven by the communal functional response f_{comm},

$$\dot{p}_{A_i} = f_{comm}\{\dot{p}_{Am}\} s_{M_i} L_i^2. \tag{18}$$

Once assimilation was known, all other energy fluxes and dynamics of the state variables followed the DEB theory. Using auxiliary parameters (Table 2), the abstract DEB variables were translated into biological metrics, i.e. physical length, weight, and fertility (Table 1). Length and weight were then used to calculate Fulton's condition index (K), a widely used indicator of fish well-being (Nash et al., 2006; Ricker, 1975), as the ratio of the physical weight (g) to cubed length (cm^3), scaled by a factor 100 to bring the value close to unity,

$$K = 100 \frac{W_w}{L_w^3}. \tag{19}$$

2.4 Fishing mortality

Fishing was incorporated through an instantaneous fishing mortality rate added to the natural mortality. The total mortality probability, M, of each fish was calculated as

$$M = 1 - e^{-(\dot{M}_n + \dot{M}_f)\Delta t} \tag{20}$$

where $\dot{M}_n$ represents a life-stage specific natural mortality rate, accounting for both age-related and predation mortality (Table 3), $\dot{M}_f$ represents instantaneous fishing mortality rate, and Δt is the model time-step equal to $1/365$ year, i.e. 1 day. The fishing mortality

was applied to adult individuals only, i.e. the stock. Survival was treated as a stochastic process complying with the calculated mortality probability. Population was assumed to have collapsed when the average population size fell below 10% of the initial stock size.

Table 3: Mortality parameters for European pilchard, taken from ICES (2019). Mortality of the eggs is expressed as a proportion of total amount of released eggs; mortalities for other life stages are instantaneous mortality rates, denoted by the dot as per DEB convention.

Life stage	**Symbol**	**Value**	**Unit**
Eggs[†]	M_{egg}	0.998	%
Juveniles	$\dot{M}_j$	1.071	/y
Adults	$\dot{M}_a$	0.61 [‡] / 0.38	/y
Fishing	$\dot{M}_f$	range from 0 to 4	/y

[†] Egg mortality is applied as a one-time mortality event prior the hatch (see Supplement S2.7, *Hatching*)
[‡] Mortality of early adults, i.e up to 1 year post maturation.

2.5 Simulations

Through its BehaviorSpace tool, NetLogo enables automated setup of multiple simulations, each with different combination of predefined inputs. We simulated two levels of food availability - high and low - to represent two environmental carrying capacity scenarios. Within each scenario we run a set of simulations by applying a range of instantaneous fishing mortality rates from 0 to 4 per year, with a step of 0.1; in total, 41 simulations for each of the two carrying capacity scenarios. Each simulation started with a 15-year period without fishing to minimize effects of transients by allowing the population to approach the non-fishing steady state.

Following the initial non-fishing period, a simulation-specific constant fishing mortality was applied to the population for a minimum duration of another 25 years (40 years in total; Figure 2). Regardless of the fishing mortality, the total daily food availability, and hence carrying capacity, was constant throughout the simulations. The simulations were continued until the population reached a new steady state criteria or went extinct. The steady state criteria was indicated when a 2-year average value of f_{comm} coincided with the 10-year average, i.e. the two averages did not differ more than ± 1%.

Initial population for each simulation consisted of adults only, respecting average sex ratio $^M/_F = 1$ (Keznine et al., 2020; Mustač & Sinovčić, 2010), and with population size set close to the equilibrium value of a non-fished population. The initial physiological traits

of individuals were distributed around the average size, weight, reserve, and maturity of an average adult. Please see Supplement S2.5 for details on model initialization.

Each submodel was run once per simulation time-step (a day). The *Spawning* submodel ran during spawning season, set to be 90 consecutive days per year (days 180 - 270). The detailed algorithm and the description of each submodel are given in the Supplement S2.3 and S2.7, respectively.

2.6 Outputs and analysis

Individual-level traits (length, weight, condition index, energy reserve, and age at sexual maturation), and population-level traits (abundance, stock biomass, and fished biomass), were recorded at each time-step. All recorded data was processed, analysed and visualised using MATLAB R2017a software. The significance of the impact of environmental carrying capacity on both individual and population traits of surviving populations was tested using Wilcoxon signed-rank test with the level of significance of 0.01. The regression visualized in the resulting figures is a robust moving average applied to simulated steady state values, obtained using weighted linear least squares and a 2^{nd} degree polynomial model, i.e. `smooth` function with `rloess` method and span of 0.7. For the purpose of visualization, we applied a log_{10} transformation to the population abundance results.

3 Results

The composite DEB-IBM model realistically simulates life history traits and captures population dynamics of European pilchard. All physiological traits observed at the steady state are within reported ranges. Fishing mortality affects population size and, therefore, level of intraspecific competition for food. The competition, in turn, affects individual-level traits. Environmental carrying capacity has significant effect on population traits ($p < 10^{-6}$ for all population traits) but, surprisingly, effects on the individual traits are not significant ($p = 0.261$ for condition index; $p = 0.202$ for time at sexual maturation; $p = 0.079$ for weight; $p = 0.013$ for length; $p = 0.111$ for energy reserve). The same trends, and range of values, are observed when the alternative food dynamics approach (chemostat type) is applied (Supplement S3). Simulations for gilthead seabream (Supplement S1) yield the same trends as for European pilchard. Comparisons below include only surviving populations.

3.1 Effects of fishing

The highest sustainable fishing mortality of European pilchard, i.e. the maximal fishing mortality that does not lead to a population collapse, F_{ms}, is similar for both environmental carrying capacity scenarios, 3.7 and 3.6 per year respectively for high and low carrying capacity (Figure 3). Average condition index, weight, and length of fish are positively correlated with increase of fishing mortality (Figure 3a and 3c). For both high and low carrying capacity, the highest condition index, 0.94 and 0.93, respectively, is recorded at F_{ms}. Age at sexual maturation decreases as the fishing mortality increased, ranging from approx. 270 days in non-fished populations, to 150 days at F_{ms} (Figure 3e). Stock size is negatively correlated with fishing mortality (Figure 3b). Stock biomass stagnates up to a fishing mortality of 2.5 per year, and decreases rapidly therafter (Figure 3d). Non-fished stock size is around 7 times higher, and the stock biomass around 1.6 times higher, compared to the respective values at F_{ms}, for both carrying capacity scenarios. The fished biomass increases with harvesting up to a fishing mortality of 3.1 and 3 per year, and rapidly decreases above 3.4 and 3.2 (Figure 3f), for high and low carrying capacity scenario, respectively. Fluctuations of both individual- and population-level traits are noticeably greater for the non-fished population, indicating that introduction of fishing mortality has a stabilizing effect on the population dynamics (Figure 2).

3.2 Impact of environmental carrying capacity

The environmental carrying capacity dictates the maximal number of individuals a population can maintain. Expectedly, higher carrying capacity results in higher abundances. Within each carrying capacity scenario, abundance decreases as fishing mortality increases (Figure 3b), resulting in equivalent relationship between individual traits and abundance in both scenarios (Figure 4). The average functional response (food availability per individual), condition index, and weight are inversely correlated with the stock size. Highest condition index is recorded at low abundance, while the lowest condition index of 0.56 is recorded at a high abundance, for both carrying capacity scenarios (Figure 4b). Weight decreases from approx. 56 to 9 grams as the stock size increases (Figure 4c). Age at sexual maturation increases as the stock size increases due to higher intraspecific competition for food (Figure 4d). Consistently with observations that maturity is mostly reached within the first year (Froese & Pauly, 2022; Véron et al., 2020), age at sexual maturation ranges from 150 at low to about 300 days at high abundance, in both carrying capacity scenarios.

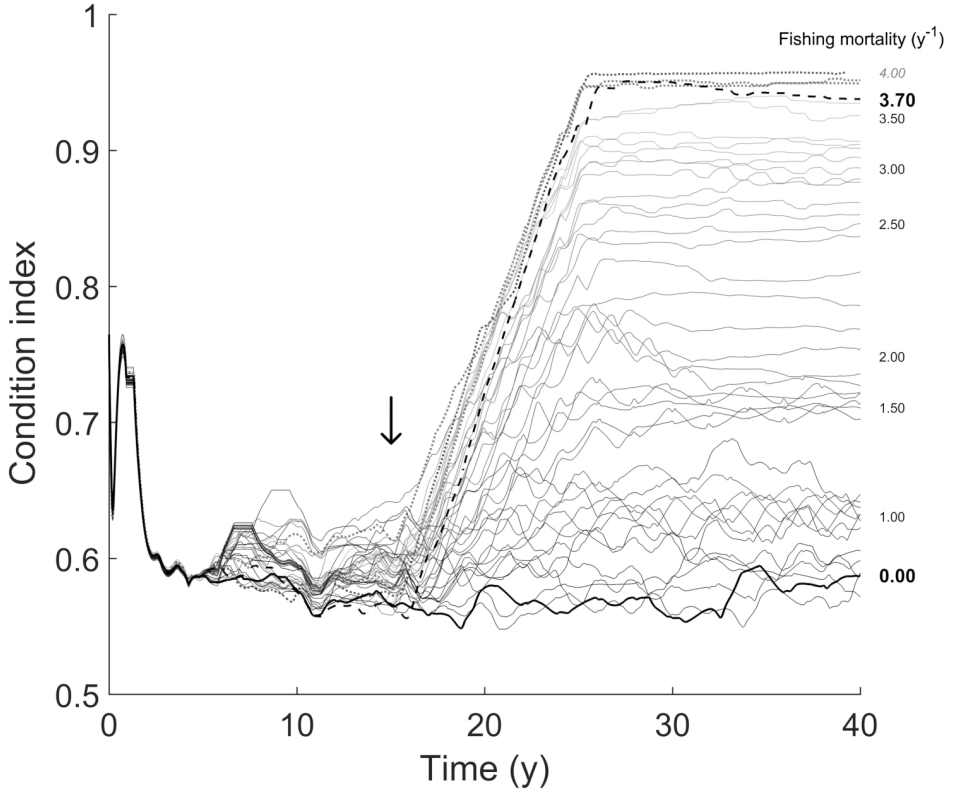

Figure 2: Condition index of European pilchard at different fishing mortalities for high carrying capacity scenario. Lines correspond to a 10-year average condition index of adult females. Thick solid line represents the non-fished population, dashed line corresponds to F_{ms}, the maximum simulated sustainable fishing mortality (3.7 per year). Dotted lines are simulation at fishing mortality rates $\geq$3.8 per year, resulting in population collapse (decrease of the average population size below 10% of the initial stock size). The arrow indicates introduction of fishing mortality at the end of year 15 of the simulation. Labels on the right represent instantaneous fishing mortality rates corresponding to the respective lines; note that only every 5^{th} simulation is labeled, and fishing mortalities causing population collapse are indicated in italic.

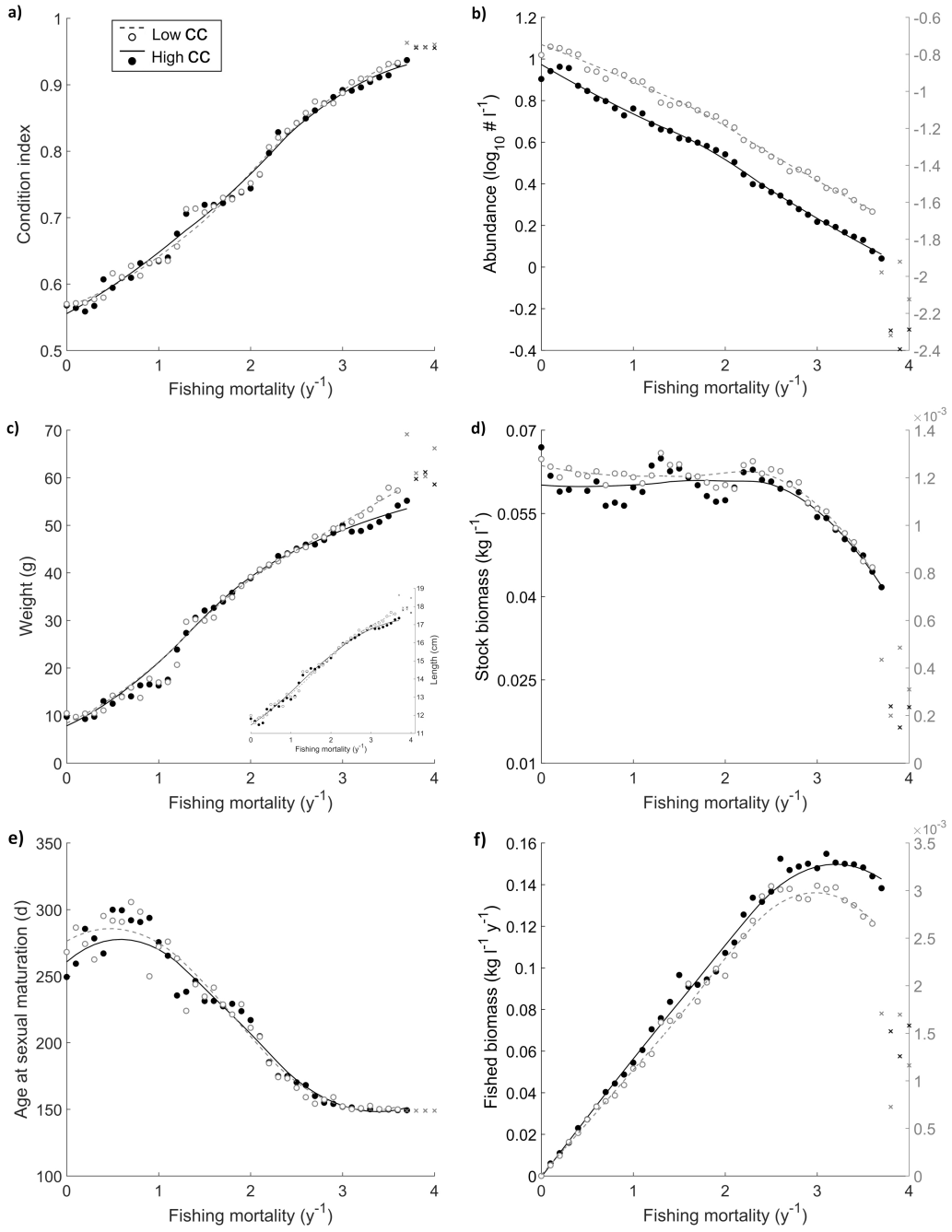

Figure 3: Impact of fishing mortality on individual-level (left panels) and population-level (right panels) traits of adult European pilchard for high and low environmental carrying capacity. Markers represent a 10-year average recorded at the end of each simulation, and the lines are moving average regressions, applied to the non-collapsed populations only (circles); the X markers correspond to the collapsed populations (average population size below 10% of the initial stock size). Right y-axes on panels (b), (d), and (f) correspond to the low carrying capacity scenario. Individual condition index (a), weight (c), and length (c - insert) increase, and the time to reach sexual maturation (e) decreases with fishing mortality for both carrying capacity scenarios. Stock size (b) decreases with fishing mortality for both scenarios, while stock biomass stagnates up to a fishing mortality of 2.5 per year and decreases thereafter (d). Fished biomass (f) increases up to a fishing mortality of around 3 per year, and decreases afterwards. Note that log_{10} scale is used for the visualization of abundance in panel (b).

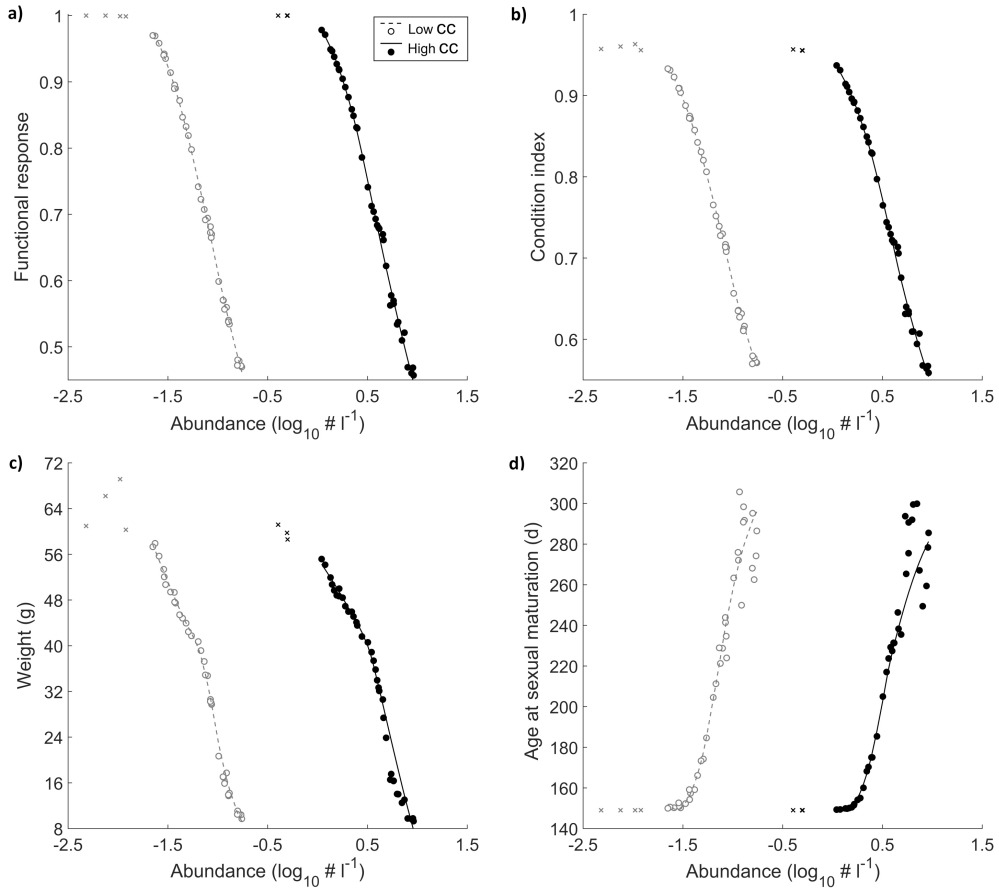

Figure 4: Functional response and individual-level traits of adult European pilchard at a steady state, for low and high carrying capacity scenarios, as functions of adult fish abundance (stock size). Markers represent a 10-year average recorded at the end of each simulation, and the lines are moving average regressions, applied to the non-collapsed populations only (circles); the X markers correspond to the collapsed populations (average population size below 10% of the initial stock size). Functional response (a), condition index (b), and weight (c) decrease, while age at sexual maturation (d) increases with abundance, for both carrying capacity scenarios. Note the abundance (x-axis) is log_{10} transformed for easier visualization.

4 Discussion

Interdependencies between condition index and stock size have long been overlooked and/or misinterpreted by managers and decision-makers in fisheries and conservation. For example, in the session on the assessment of European anchovy and sardine in the Adriatic Sea (GFCM, 2022b) fish condition is not even mentioned. Furthermore, statements like "(...) size and age structure showed no improvement of the stock in terms of ecological state, *despite* an increase in body condition." (GFCM 2018, p24) and "(...) management measures need to ensure that if size and condition increase again, the fishing activity would not increase too much in order to allow the stock to recover." (GFCM 2022a, p16) clearly indicate the common wisdom that higher condition index implies better stock status. Our results directly contradict such common wisdom - indeed, we suggest low condition index indicates population size close to, or above, the carrying capacity of the environment, and high condition index indicates overfished stock.

Using a composite Dynamic Energy Budget - Individual-based model (DEB-IBM), we show that condition index of an individual can reflect the status of its population. The finding relies on the assumption of a constant carrying capacity in a food-limited population. In such populations, a fixed amount of resources is shared among all individuals, thus determining the maximum population size a habitat can sustain (Sayre, 2008). Individual food availability that ultimately dictates condition index, therefore, depends primarily on the competition between individuals, i.e. the number of individuals and their capacity for assimilation of food.

Our simulations of variable fish exploitation, combined with a range of realistic fishing mortalites, indicate that the average individual condition index of fish increases with increased fishing mortality, and with lower abundance. Opposite, as a consequence of increased intraspecific competition for available resources, condition index decreases when the population size approaches the environmental carrying capacity, regardless of the absolute value of the carrying capacity.

Condition index therefore provides an estimate of the stock size relative to the environmental carrying capacity, without the need to actually know the carrying capacity, or the current stock size. Avoiding the need for carrying capacity and stock estimates could simplify decision-making: estimating the absolute carrying capacity is a complex process

that has not been standardized despite frequent use (Chapman & Byron, 2018; Shaffer, 1981), and estimating stock size is a data-intensive procedure wrought with uncertainties (Headley, 2020; Lynch et al., 2018).

We use a simple food dynamics where each day a fixed amount of food is available to the whole population. Individuals, therefore, compete for food: increase in population size reduces food availability per individual. Lower food availability then leads to lower reserves and reduced reproduction, leading to density-dependent response of condition index. The trend should be observed in all food-limited environments with intraspecific competition for food. Repeating the simulations with an alternative - chemostat - food dynamics validates the mechanism: the observed trends are the same (Supplement S3).

Because the competition for resources among individuals of the same species is universal (Ward et al., 2006), qualitative correlation between condition index and population size relative to the environmental carrying capacity is also a general feature, rather than a function of species-specific parameters. Condition index only increases if increase in weight overtakes the increase in volume (length cubed). This is, indeed, always the case, simply because every organism exposed to higher food will get fatter, i.e. it will have more energy reserves relative to its size, thus contributing more to the weight. This concept is one of the chief requirements for any energetics-based model, including DEB (Kooijman, 2020). Furthermore, mechanisms incorporated into DEB and IBM are general, implying that the observed relationships between condition index and population-level indicators are general, too. We validate the generality by showing the same relationships emerging for two biologically and ecologically significantly different species - a small pelagic European pilchard vs. a demersal predator gilthead seabream.

Our results depend on the idea that more food supports more energy reserves, and faster growth, which is independent of energy allocation to growth and somatic maintenance, represented through parameter κ. Both of our model species are characterized with high κ value, a typical value for ray-finned fish in general: 68% of 953 parameterized ray-finned fish have κ higher than 0.8; of those, more than half have $\kappa > 0.94$ (AmP, 2023). Potentially, low-κ species might exhibit less pronounced patterns presented in this study simply because their range of condition indices might be lower, and spawning-related fluctuations of the condition index higher.

Density dependence plays a significant role in population dynamics and individual

condition. Generally, density dependence is introduced through a negative effect on reproduction, growth, and/or survival that increases with population size (van Gemert & Andersen, 2018). Indeed, the root cause of the density dependence is intraspecific competition for resources, often food (Amundsen et al., 2007; Hazlerigg et al., 2012) - a mechanism inherently captured by our approach, without the need for ad-hoc assumptions and additional parameters.

Other density-dependence mechanisms could, however, also be active. For example, density-dependent mortality (Rose et al., 2001; Stige et al., 2019) or cannibalism (Canales et al., 2020; Ricard et al., 2016) could limit population size significantly below the one determined by total food availability. If factors other than food control population growth, the population might never reach the state where competition for food is strong enough to impact individual energy status and, consequently, individual traits such as condition index. In such cases, the condition index would not be a good indicator of population size relative to the carrying capacity.

Though in principle it could, the model does not account for seasonal fluctuation of environmental variables known to influence the physiological condition and reproductive output of the organism (Mazumder et al., 2016; Morgan et al., 2010). For example, temperature is seasonal and affects physiological rates, but is constant in all simulations. Our DEB-IBM model could account for temperature fluctuations, if needed: the fluctuations are captured by a temperature-dependent coefficient that affects metabolic rates of assimilation, energy conductance, and maintenance (Kooijman, 2010). Temperature fluctuations, however, do not affect the feedback between food and population size, thus would not change the general patterns related to the condition index and population size we are focusing on.

Contrary to the field observations, our results indicate both weight and length increase with fishing mortality. This stems from the (i) non-selective exploitation of the stock where any adult fish, regardless of the size, has equal chance of being caught, and (ii) the fact that no evolutionary considerations were incorporated in the model. In reality however, fishermen tend to preferentially catch larger fish. Also, fishing is a major driver of evolutionary changes of heavily exploited stocks resulting in decrease of age and size at sexual maturation (Swain, 2011).

Our model could address both size-selective fishing pressure, and the emerging evolu-

tionary changes. Currently, weight and length are average values of a steady state population where, with increased fishing mortality, non-caught individuals have more food *per capita*, allowing them to reach larger size and weight. Imposing (increased) fishing mortality on larger individuals only, would reduce the average length. The average weight of the individuals - limited by their size - would also decrease. Nevertheless, increased food availability (due to reduced competition) would still allow for larger energy reserves, thus increasing weight relative to the size. Therefore, average condition index would reflect food availability even as average size changes, providing an estimate independent of mechanisms affecting the average fish size.

If needed, evolutionary considerations could be incorporated into our model through introduction of individual-specific parameters. Rather than using a single DEB parameter value for all individuals, each individual could have a different parameter value drawn from a distribution, and be tracked using inheritance rules. However, additional genealogical data would be needed to validate results. Including evolutionary considerations would most likely favor fish reaching maturity earlier and, therefore, at a smaller size - thus, consistent with observations, driving the average size down. The condition index would, however, remain a reliable estimate of stock status as it would not be affected by the faster maturation and/or growth.

Survival of any exploited stock is affected by a combination of natural and fishing mortalities. Fishing mortality in our model varies between simulations, while natural mortality accounting for age-related and predation mortalities is kept constant. Because mortality rates are *linearly* combined, in principle they are interchangeable. For example, increasing predation mortality while decreasing fishing mortality by the same value does not change simulation outputs. Because our conclusions actually depend on total mortality, the level of natural mortality does not affect the qualitative results; it merely changes the fraction of total mortality that can be attributed to fishing. Hence, regardless of the level of natural mortality, condition index will increase as fishing mortality increases. We explicitly model fishing mortality to record the number and biomass of caught fish; if the distinction between caught and naturally died fish is not important, using a single parameter - the total mortality - would suffice.

Low fisheries yields can result from overfishing a small stock, or underfishing a large stock (Francis & Shotton, 1997; Hart, 2013); we suggest condition index can help dis-

tinguish between these two alternatives without the need for stock size or fishing effort estimates. If the condition index of caught fish is high, the population size is much lower than the carrying capacity; the stock is therefore most likely overfished, and could be under an imminent threat of a collapse. Conversely, if the condition index is low, the population size is near or above the carrying capacity; fishing could therefore safely be increased.

Note that seasonal fluctuations of condition index need to be taken into the account during the analysis. Even in ecosystems with a constant environmental carrying capacity, reproduction can cause seasonal fluctuations in condition index: seasonal reproduction results in reduction of weight (and therefore condition index) during the spawning season. Such fluctuations are inherently included in the DEB-IBM.

If, even after accounting for seasonal fluctuations of the condition index, population estimates clash with the stock status estimates from the condition index, the assumption of a food-limited environmental carrying capacity should be verified. For example, some studies report that decrease in population size coincides with the reduction of fish growth and condition. Morgan et al. (2018) presented this for northern cod, indicating that low growth and condition could be related to reduced productivity, causing population decline and delaying population rebuilding. At the same time, however, they report that population of an important cod prey, capelin, was also declining to very low levels. Because both fish are highly exploited, the source of the cod population decline and its low condition might therefore be the overfishing of its prey - causing decreased carrying capacity and starvation-induced mortality (Mullowney & Rose, 2014; Regular et al., 2022) - rather than fisheries of cod itself. Here, advice to reduce cod fishing due to its low condition index would not have much benefit for the recovery of its population, and the starvation-induced mortality would persist.

In such cases (of e.g. predatory fish), bad condition would not indicate overcrowding relative to its pre-industrial status, but *would* indicate overcrowding relative to the new, significantly lower carrying capacity set by overfishing of the prey. Increasing fishing pressure on the predator could then increase extinction risk despite the fact that the population reached (the new, lower) environmental carrying capacity. Combining the information on condition of both predator and prey species could elucidate the true source of each populations' decline, and could be beneficial in multi-species management to

determine how to adapt fishing efforts on each species. For example, management may consider protecting the prey while allowing fishing of the predator (at a reduced rate), so both the prey and the predator can recover. Indeed, all species interact with the ecosystem (MSC 2018); these interactions should not be overlooked in management. Hence, the condition index offers supplementary information, but its interpretation has to be carefully integrated once the shifts of the whole ecosystem are clarified.

While additional research and empirical validation is needed before we can consistently rely on the condition index as a measure of stock status, our findings can already be integrated into current decision-making, as suggested in Figure 5. The approach gives priority to the standard stock assessment protocol, which uses field data - catch, abundance, and biology - to drive stock assessment models (Lynch et al., 2018). Condition index - calculated from the same data at marginal additional cost - can then be used as an inexpensive and rapid validation tool:

1. Stock status is estimated to be poor, and the condition index is high. The two independent estimates are consistent, and standard assessment is validated.

2. Stock status is estimated to be good, and the condition index is low. The two independent estimates are consistent, and standard assessment is validated.

3. Stock status is estimated to be poor, and the condition index is low. The two independent estimates are *not* consistent, and decision-making could benefit from additional research.

4. Stock status is estimated to be good, and the condition index is high. The two independent estimates are *not* consistent, and decision-making could benefit from additional research.

Additional research, following confirmation that the population is indeed food-limited, can include assessment of environmental factors (e.g. habitat, prey, exposure to pathogens) or human impact (illegal and unreported fishing) (Link et al., 2020). One could also, for example, extend analysis of the species physiology by analysing bio-markers (Brosset et al., 2021), use food web knowledge to identify changes in the ecosystem dynamics (Eero et al., 2021), and/or perform an overall in-depth analysis of major mechanisms impacting living marine resource of interest (Link et al., 2020).

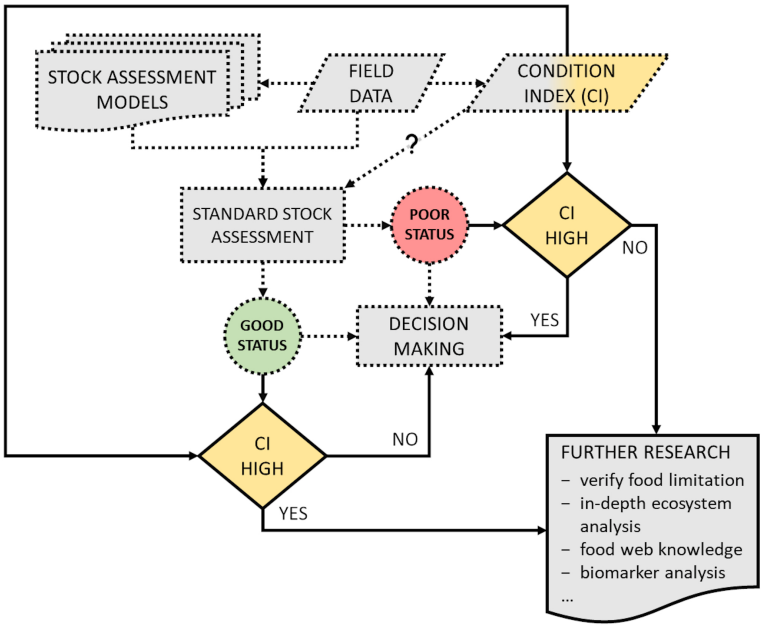

Figure 5: Suggested integration of condition index into decision-making. Dashed lines depict simplified current approach; question mark indicates current limited and/or questionable use of condition index (CI). Solid lines indicate the new role of condition index as a supplementary information to the standard stock assessment. Field data drive stock assessment models, and combined information is used for stock assessment. Rather than used directly in further decision-making, the standard results can now be verified against the condition index obtained from the field data. If the two independent assessments agree (poor stock status + high condition index, or good stock status + low condition index), no intervention is needed. If, however, the two assessments differ (poor stock status + low condition index, or good stock status + high condition index) decision making could benefit from additional research into reasons behind the discrepancies.

Our study was guided by, and has confirmed, the premise that combining measurements at more than one level of biological organization can provide complementary information for fisheries management and conservation decision-making. To our knowledge, only Arismendi et al. (2011) and Ordines et al. (2019) performed simultaneous analysis of fish condition index and abundance, aiming to respectively determine a correlation useful for rapid stock assessment, and diagnose recruitment overfishing. Consistently with our results, they also observe negative correlation of condition index with stock size. Both studies were based exclusively on empirical data, without explicit mechanistic understanding of the correlation. By using a composite DEB-IBM modelling approach, we implement the underlying physiological processes to analyse and explain the mechanisms behind the correlation, and generalize the finding. Condition index is therefore revealed as a simple and general yet powerful metric, holding more information about the population than previously thought.

5 Conclusions

Condition index is a powerful, yet inexpensive indicator of the status of the population. We show that condition index can (i) indicate how stock size compares to the food-limited environmental carrying capacity of the species, thus helping differentiate under-fishing from imminent stock collapse, and (ii) track population trends. Some ambiguities, however, remain. For example, processes other than food limitation (e.g. disease, variable primary productivity, season) could be driving condition index dynamics, or the population may not be limited by food.

We suggest condition index analysis should be incorporated as an important part of stock assessment process, but (at least for now) used mainly as a supplementary information alongside standard stock assessment methods (Figure 5). Conflicting information between the two assessments indicates possibility of additional factors affecting stock dynamics, and the need for further analysis. Hence, even though additional research is warranted, our work shows that condition index can already directly contribute to decision-making in fisheries, and marine resource management and conservation in general.

Author Contributions

IH: formal analysis, investigation, data curation, software, writing – original draft, writing - review and editing. LB: conceptualization, methodology, writing - review and editing. TK: conceptualization, methodology, supervision, funding acquisition, writing – original draft, writing - review and editing.

Acknowledgments

The authors would like to thank Nina Marn and Jasminka Klanjšček for helpful advice during development of the DEB-IBM model. IH was funded by the Croatian Science Foundation (HRZZ) through *Young Researchers' Career Development Project*, DOK-2018-09-4671. This work has been fully supported through the HRZZ grant IP-2018-01-3150-AqADAPT to TK.

Conflict of Interest Statement: All authors declare no conflict of interest.

Data Availability Statement: The data and code underlying the findings of this study are openly available in Zenodo, `https://doi.org/10.5281/zenodo.7569367`.

References

Ahti, P. A., Uusi-Heikkilä, S., Marjomäki, T. J., & Kuparinen, A. (2021). Age is not just a number — mathematical model suggests senescence affects how fish populations respond to different fishing regimes. *Ecology and Evolution*, *11*, 13363–13378. https://doi.org/10.1002/ece3.8058.

AmP (2023). Add-my-Pet collection. https://www.bio.vu.nl/thb/deb/deblab/add_my_pet/species_list.html. Accessed on 30.01.2023.

Amundsen, P.-A., Knudsen, R., & Klemetsen, A. (2007). Intraspecific competition and density dependence of food consumption and growth in Arctic charr. *Journal of Animal Ecology*, *76*, 149–158. https://doi.org/10.1111/j.1365-2656.2006.01179.x.

Anderson, R. O., & Neumann, R. M. (1996). Length, weight, and associated structural indices. In *Fisheries techniques, 2nd Ed* (pp. 447–482). Bethesda, MD: American Fisheries Society.

Arismendi, I., Penaluna, B., & Soto, D. (2011). Body condition indices as a rapid assessment of the abundance of introduced salmonids in oligotrophic lakes of southern Chile. *Lake and Reservoir Management*, *27*, 61–69. https://doi.org/10.1080/07438141.2010.536617.

Bavčević, L., Petrović, S., Karamarko, V., Luzzana, U., & Klanjšček, T. (2020). Estimating fish energy content and gain from length and wet weight. *Ecological Modelling*, *436*, 109280. https://doi.org/10.1016/j.ecolmodel.2020.109280.

Beaudouin, R., Goussen, B., Piccini, B., Augustine, S., Devillers, J., Brion, F., & Péry, A. R. (2015). An individual-based model of zebrafish population dynamics accounting for energy dynamics. *PloS One*, *10*, e0125841. https://doi.org/10.1371/journal.pone.0125841.

Blackwell, B. G., Brown, M. L., & Willis, D. W. (2000). Relative weight (Wr) status and current use in fisheries assessment and management. *Reviews in Fisheries Science*, *8*, 1–44. https://doi.org/10.1080/10641260091129161.

Bolin, J. A., Schoeman, D. S., Evans, K. J., Cummins, S. F., & Scales, K. L. (2021). Achieving sustainable and climate-resilient fisheries requires marine ecosystem forecasts to include fish condition. *Fish and Fisheries*, *22*, 1067–1084. https://doi.org/10.1111/faf.12569.

Brosset, P., Cooke, S. J., Schull, Q., Trenkel, V. M., Soudant, P., & Lebigre, C. (2021). Physiological biomarkers and fisheries management. *Reviews in Fish Biology and Fisheries*, *31*, 797–819. https://doi.org/10.1007/s11160-021-09677-5.

Canales, T. M., Delius, G. W., & Law, R. (2020). Regulation of fish stocks without stock–recruitment relationships: The case of small pelagic fish. *Fish and Fisheries*, *21*, 857–871. https://doi.org/10.1111/faf.12465.

Chapman, E. J., & Byron, C. J. (2018). The flexible application of carrying capacity in ecology. *Global Ecology and Conservation*, *13*, e00365. https://doi.org/10.1016/j.gecco.2017.e00365.

Chen, Z., Bigman, J., Xian, W., Liang, C., Chu, E., & Pauly, D. (2022). The ratio of length at first maturity to maximum length across marine and freshwater fishes. *Journal of Fish Biology*, *101*, 400–407. https://doi.org/10.1111/jfb.14970.

Costello, C., Ovando, D., Hilborn, R., Gaines, S. D., Deschenes, O., & Lester, S. E. (2012). Status and solutions for the world's unassessed fisheries. *Science*, *338*, 517–520. https://doi.org/10.1126/science.1223389.

De Roos, A. M., Metz, J. A. J., Evers, E., & Leipoldt, A. (1990). A size dependent predator-prey interaction: who pursues whom? *Journal of Mathematical Biology*, *28*, 609–643. https://doi.org/10.1007/BF00160229.

DeAngelis, D. L., & Mooij, W. M. (2005). Individual-based modeling of ecological and evolutionary processes. *Annual Review of Ecology, Evolution, and Systematics*, *36*, 147–168. https://doi.org/10.1146/annurev.ecolsys.36.102003.152644.

Dennis, D., Plagányi, É., Van Putten, I., Hutton, T., & Pascoe, S. (2015). Cost benefit of fishery-independent surveys: are they worth the money? *Marine Policy*, *58*, 108–115. https://doi.org/10.1016/j.marpol.2015.04.016.

Eero, M., Dierking, J., Humborg, C., Undeman, E., MacKenzie, B. R., Ojaveer, H., Salo, T., & Köster, F. W. (2021). Use of food web knowledge in environmental conservation and management of living resources in the Baltic Sea. *ICES Journal of Marine Science*, *78*, 2645–2663. https://doi.org/10.1093/icesjms/fsab145.

FAO (2022). Fishery and Aquaculture Statistics. Global production by production source 1950-2020 (FishStatJ). In *FAO Fisheries and Aquaculture Division [online]*. Rome: FAO Fisheries and Aquaculture Department. Updated 2022. FishStatJ software available at: https://www.fao.org/fishery/en/topic/166235.

Fenberg, P. B., & Roy, K. (2008). Ecological and evolutionary consequences of size-selective harvesting: how much do we know? *Molecular ecology*, *17*, 209–220. https://doi.org/10.1111/j.1365-294X.2007.03522.x.

Francis, R., & Shotton, R. (1997). "Risk" in fisheries management: a review. *Canadian Journal of Fisheries and Aquatic Sciences*, *54*, 1699–1715. https://doi.org/10.1139/f97-100.

Froese, R., & Pauly, D. (2022). Fishbase: *Sardina pilchardus*. https://www.fishbase.se/summary/sardina-pilchardus.html. Accessed on 2.11.2022.

GBIF Secretariat (2021). GBIF Backbone Taxonomy. https://doi.org/10.15468/39omei. Accessed via https://www.gbif.org/species/2413224 [*Sardina pilchardus* (Walbaum, 1792)] on 03.03.2022.

van Gemert, R., & Andersen, K. H. (2018). Challenges to fisheries advice and management due to stock recovery. *ICES Journal of Marine Science*, *75*, 1864–1870. https://doi.org/10.1093/icesjms/fsy084.

GFCM (2018). Report of the Working Group on Stock Assessment of Small Pelagic species (WGSASP). Scientific Advisory Committee (SAC), The General Fisheries Commission for the Mediterranean (GFCM). Technical meeting, FAO Rome, Italy, November.

GFCM (2022a). Report of the Working Group on Stock Assessment of Small Pelagic species (WGSASP). Scientific Advisory Committee (SAC), The General Fisheries Commission for the Mediterranean (GFCM). Online technical meeting, FAO Rome, Italy, January.

GFCM (2022b). Report of the Working Group on Stock Assessment of Small Pelagic Species (WGSASP) session on the assessment of European anchovy and sardine in the Adriatic Sea. Scientific Advisory Committee (SAC), The General Fisheries Commission for the Mediterranean (GFCM). Online technical meeting, FAO Rome, Italy, May.

Goedegebuure, M., Melbourne-Thomas, J., Corney, S. P., McMahon, C. R., & Hindell, M. A. (2018). Modelling southern elephant seals *Mirounga leonina* using an individual-based model coupled with a dynamic energy budget. *PloS One*, *13*, e0194950. https://doi.org/10.1371/journal.pone.0194950.

Grimm, V., Ayllón, D., & Railsback, S. F. (2016). Next-generation individual-based models integrate biodiversity and ecosystems: yes we can, and yes we must. *Ecosystems*, *20*, 229–236. https://doi.org/10.1007/s10021-016-0071-2.

Grimm, V., Berger, U., Bastiansen, F., Eliassen, S., Ginot, V., Giske, J., Goss-Custard, J., Grand, T., Heinz, S. K., Huse, G., Huth, A., Jepsen, J. U., Jørgensen, C., Mooij, W. M., Müller, B., Pe'er, G., Piou, C., Railsback, S. F., Robbins, A. M. et al. (2006). A standard protocol for describing individual-based and agent-based models. *Ecological Modelling*, *198*, 115–126. https://doi.org/10.1016/j.ecolmodel.2006.04.023.

Grimm, V., Berger, U., DeAngelis, D. L., Polhill, J. G., Giske, J., & Railsback, S. F. (2010). The ODD protocol: a review and first update. *Ecological Modelling*, *221*, 2760–2768. https://doi.org/10.1016/j.ecolmodel.2010.08.019.

Grimm, V., & Railsback, S. F. (2005). *Individual-based modeling and ecology*. Princeton University Press. EBook published in 2013.

Grimm, V., Railsback, S. F., Vincenot, C. E., Berger, U., Gallagher, C., DeAngelis, D. L., Edmonds, B., Ge, J., Giske, J., Groeneveld, J., Johnston, A. S., Milles, A., Nabe-Nielsen, J., Polhill, G., Radchuk, V., Rohwäder, M.-S., Stillman, R. A., Thiele, J. C., & Ayllón, D. (2020). The ODD protocol for describing agent-based and other simulation models: A second update to improve clarity, replication, and structural realism. *Journal of Artificial Societies and Social Simulation*, *23*, 7. https://doi.org/10.18564/jasss.4259.

Hart, D. R. (2013). Quantifying the tradeoff between precaution and yield in fishery reference points. *ICES Journal of Marine Science*, *70*, 591–603. https://doi.org/10.1093/icesjms/fss204.

Hazlerigg, C. R., Lorenzen, K., Thorbek, P., Wheeler, J. R., & Tyler, C. R. (2012). Density-dependent processes in the life history of fishes: evidence from laboratory populations of zebrafish *Danio rerio*. *PLoS One*, *7*, e37550. https://doi.org/10.1371/journal.pone.0037550.

Headley, M. (2020). *Determining the status of fish stocks in data-poor environments and multispecies fisheries*. Winnipeg, Manitoba, Canada: The International Institute for Sustainable Development.

ICES (2019). Working Group on Southern Horse Mackerel, Anchovy and Sardine (WGHANSA). *ICES Scientific Reports*, *1:34*, 653p. https://doi.org/10.17895/ices.pub.4983.

Jusup, M., Sousa, T., Domingos, T., Labinac, V., Marn, N., Wang, Z., & Klanjšček, T. (2017). Physics of metabolic organization. *Physics of life reviews*, *20*, 1–39. https://doi.org/10.1016/j.plrev.2016.09.001.

Keznine, M., Analla, M., Aksissou, M., & El Meraoui, A. (2020). The reproduction and growth of the sardine *Sardina pilchardus* in West Mediterranean, Morocco. *Egyptian Journal of Aquatic Biology and Fisheries*, *24*, 303–319. https://doi.org/10.21608/ejabf.2020.98433.

Kooijman, S., Pecquerie, L., Augustine, S., & Jusup, M. (2011). Scenarios for acceleration in fish development and the role of metamorphosis. *Journal of sea research*, *66*, 419–423. https://doi.org/10.1016/j.seares.2011.04.016.

Kooijman, S. A. (2020). The standard dynamic energy budget model has no plausible alternatives. *Ecological Modelling*, *428*, 109106. https://doi.org/10.1016/j.ecolmodel.2020.109106.

Kooijman, S. A. L. M. (2010). *Dynamic Energy Budget theory for metabolic organisation*. Cambridge: Cambridge University Press.

Kooijman, S. A. L. M. (2014). Metabolic acceleration in animal ontogeny: an evolutionary perspective. *Journal of Sea Research*, *94*, 128–137. https://doi.org/10.1016/j.seares.2014.06.005.

Lika, K., Kearney, M. R., Freitas, V., van der Veer, H. W., van der Meer, J., Wijsman, J. W., Pecquerie, L., & Kooijman, S. A. L. M. (2011). The "covariation method" for estimating the parameters of the standard dynamic energy budget model I: Philosophy and approach. *Journal of Sea Research*, *66*, 270–277. https://doi.org/10.1016/j.seares.2011.07.010.

Link, J. S., Huse, G., Gaichas, S., & Marshak, A. R. (2020). Changing how we approach fisheries: a first attempt at an operational framework for ecosystem approaches to fisheries management. *Fish and Fisheries*, *21*, 393–434. https://doi.org/10.1111/faf.12438.

Lloret, J., Faliex, E., Shulman, G., Raga, J.-A., Sasal, P., Muñoz, M., Casadevall, M., Ahuir-Baraja, A., Montero, F., Repullés-Albelda, A., Cardinale, M., Rätz, H.-J., Vila, S., & Ferrer, D. (2012). Fish health and fisheries, implications for stock assessment and management: the mediterranean example. *Reviews in Fisheries Science*, *20*, 165–180. https://doi.org/10.1080/10641262.2012.695817.

Lynch, P. D., Methot, R. D., & Link, J. S. (2018). Implementing a next generation stock assessment enterprise: an update to the noaa fisheries stock assessment improvement plan. U.S. Dep. Commer., NOAA Tech. Memo. NMFS-F/SPO-183, 127p. https://doi.org/10.7755/TMSPO.183.

Mackinson, S., Mangi, S., Hetherington, S., Catchpole, T., & Masters, J. (2017). Guidelines for Industry-Science Data Collection: Step-by-step guidance to gathering useful and useable scientific information. *Fishing into the Future report to Seafish*, 65p, June 2017.

Marques, G. M., Augustine, S., Lika, K., Pecquerie, L., Domingos, T., & Kooijman, S. A. L. M. (2018). The AmP project: Comparing species on the basis of dynamic energy budget parameters. *PLOS Computational Biology*, *14*, 1–23. https://doi.org/10.1371/journal.pcbi.1006100.

Martin, B. T., Heintz, R., Danner, E. M., & Nisbet, R. M. (2017). Integrating lipid storage into general representations of fish energetics. *Journal of Animal Ecology*, *86*, 812–825. https://doi.org/10.1111/1365-2656.12667.

Martin, B. T., Jager, T., Nisbet, R. M., Preuss, T. G., & Grimm, V. (2013). Predicting population dynamics from the properties of individuals: a cross-level test of dynamic energy budget theory. *The American Naturalist*, *181*, 506–519. https://doi.org/10.1086/669904.

Martin, B. T., Zimmer, E. I., Grimm, V., & Jager, T. (2012). Dynamic energy budget theory meets individual-based modelling: a generic and accessible implementation. *Methods in Ecology and Evolution*, *3*, 445–449. https://doi.org/10.1111/j.2041-210X.2011.00168.x.

Martinez, M., Guderley, H., Dutil, J.-D., Winger, P., He, P., & Walsh, S. (2003). Condition, prolonged swimming performance and muscle metabolic capacities of cod *Gadus morhua*. *Journal of Experimental Biology*, *206*, 503–511. https://doi.org/10.1242/jeb.00098.

Maury, O., & Poggiale, J.-C. (2013). From individuals to populations to communities: a dynamic energy budget model of marine ecosystem size-spectrum including life history diversity. *Journal of Theoretical Biology*, *324*, 52–71. https://doi.org/10.1016/j.jtbi.2013.01.018.

Mazumder, S. K., Das, S. K., Bakar, Y., & Ghaffar, M. A. (2016). Effects of temperature and diet on length-weight relationship and condition factor of the juvenile Malabar blood snapper (*Lutjanus malabaricus* Bloch & Schneider, 1801). *Journal of Zhejiang University-SCIENCE B*, *17*, 580–590. https://doi.org/10.1631/jzus.B1500251.

Morgan, M., Rideout, R., & Colbourne, E. (2010). Impact of environmental temperature on Atlantic cod *Gadus morhua* energy allocation to growth, condition and reproduction. *Marine Ecology Progress Series*, *404*, 185–195. https://doi.org/10.3354/meps08502.

Morgan, M. J., Koen-Alonso, M., Rideout, R. M., Buren, A. D., & Maddock Parsons, D. (2018). Growth and condition in relation to the lack of recovery of northern cod. *ICES Journal of Marine Science*, *75*, 631–641. https://doi.org/10.1093/icesjms/fsx166.

MSC (2018). MSC Fisheries Standard, Version 2.01. Marine Stewardship Council, London.

Mu, X., Zhang, C., Xu, B., Ji, Y., Xue, Y., & Ren, Y. (2021). Accounting for the fish condition in assessing the reproductivity of a marine eel to achieve fishery sustainability. *Ecological Indicators*, *130*, 108116. https://doi.org/10.1016/j.ecolind.2021.108116.

Mullowney, D. R., & Rose, G. A. (2014). Is recovery of northern cod limited by poor feeding? The capelin hypothesis revisited. *ICES Journal of Marine Science*, *71*, 784–793. https://doi.org/10.1093/icesjms/fst188.

Mustač, B., & Sinovčić, G. (2010). Reproduction, length-weight relationship and condition of sardine, *Sardina pilchardus* (Walbaum, 1792), in the eastern Middle Adriatic Sea (Croatia). *Periodicum biologorum*, *112*, 133–138.

Nash, R. D., Valencia, A. H., & Geffen, A. J. (2006). The origin of Fulton's condition factor — setting the record straight. *Fisheries*, *31*, 236–238.

Neumann, R. M., & Allen, M. S. (2007). Size structure. In *Analysis and interpretation of freshwater fisheries data* (pp. 375–421). Bethesda, MD: American Fisheries Society.

Nikolioudakis, N., Isari, S., Pitta, P., & Somarakis, S. (2012). Diet of sardine *Sardina pilchardus*: an 'end-to-end' field study. *Marine Ecology Progress Series*, *453*, 173–188. https://doi.org/10.3354/meps09656.

Nunes, C., Marques, G., Sousa, T., Kooijman, B., Queiros, Q., & Lefebvre, S. (2019). AmP *Sardina pilchardus*, version 2019/09/16. https://www.bio.vu.nl/thb/deb/deblab/add_my_pet/entries_web/Sardina_pilchardus/Sardina_pilchardus_res.html. Accessed on 15.11.2022.

Ordines, F., Lloret, J., Tugores, P., Manfredi, C., Guijarro, B., Jadaud, A., Porcu, C., Gil de Sola, L., Carlucci, R., Sartini, M., Isajlović, I., & Massutí, E. (2019). A new approach to recruitment overfishing diagnosis based on fish condition from survey data. *Scientia Marina*, *83*, 223–233. https://doi.org/10.3989/scimar.04950.03A.

Quinn, T. J., & Deriso, R. B. (1999). *Quantitative fish dynamics*. New York, NY, USA: Oxford University Press.

Regular, P. M., Buren, A. D., Dwyer, K. S., Cadigan, N. G., Gregory, R. S., Koen-Alonso, M., Rideout, R. M., Robertson, G. J., Robertson, M. D., Stenson, G. B., Wheeland, L. J., & Zhang, F. (2022). Indexing starvation mortality to assess its role in the population regulation of Northern cod. *Fisheries Research*, *247*, 106180. https://doi.org/10.1016/j.fishres.2021.106180.

Ricard, D., Zimmermann, F., & Heino, M. (2016). Are negative intra-specific interactions important for recruitment dynamics? A case study of Atlantic fish stocks. *Marine Ecology Progress Series*, *547*, 211–217. https://doi.org/10.3354/meps11625.

Ricker, W. E. (1975). Computation and interpretation of biological statistics of fish populations. *Bulletin of the Fisheries Research Board of Canada*, *191*, 1–382.

Rodríguez-Castañeda, J. C., Ventero, A., García-Márquez, M. G., & Iglesias, M. (2022). Spatial and temporal analysis (2009–2020) of the biological parameters, abundance and distribution of *Trachurus mediterraneus* (Steindachner, 1868) in the Western Mediterranean. *Fisheries Research*, *256*, 106483. https://doi.org/10.1016/j.fishres.2022.106483.

Rose, K. A., Cowan Jr, J. H., Winemiller, K. O., Myers, R. A., & Hilborn, R. (2001). Compensatory density dependence in fish populations: importance, controversy, understanding and prognosis. *Fish and Fisheries*, *2*, 293–327. https://doi.org/10.1046/j.1467-2960.2001.00056.x.

Sayre, N. F. (2008). The genesis, history, and limits of carrying capacity. *Annals of the Association of American Geographers*, *98*, 120–134. https://doi.org/10.1080/00045600701734356.

Schloesser, R. W., & Fabrizio, M. C. (2017). Condition indices as surrogates of energy density and lipid content in juveniles of three fish species. *Transactions of the American Fisheries Society*, *146*, 1058–1069. https://doi.org/10.1080/00028487.2017.1324523.

Shaffer, M. L. (1981). Minimum population sizes for species conservation. *BioScience*, *31*, 131–134. https://doi.org/10.2307/1308256.

Silva, A., Carrera, P., Massé, J., Uriarte, A., Santos, M., Oliveira, P., Soares, E., Porteiro, C., & Stratoudakis, Y. (2008). Geographic variability of sardine growth across the northeastern Atlantic and the Mediterranean Sea. *Fisheries Research*, *90*, 56–69. https://doi.org/10.1016/j.fishres.2007.09.011.

Sousa, T., Domingos, T., & Kooijman, S. (2008). From empirical patterns to theory: a formal metabolic theory of life. *Philosophical Transactions of the Royal Society B: Biological Sciences*, *363*, 2453–2464. https://doi.org/10.1098/rstb.2007.2230.

Stevenson, R. D., & Woods, J., William A. (2006). Condition indices for conservation: new uses for evolving tools. *Integrative and Comparative Biology*, *46*, 1169–1190. https://doi.org/10.1093/icb/icl052.

Stige, L. C., Rogers, L. A., Neuheimer, A. B., Hunsicker, M. E., Yaragina, N. A., Ottersen, G., Ciannelli, L., Langangen, Ø., & Durant, J. M. (2019). Density-and size-dependent mortality in fish early life stages. *Fish and Fisheries*, *20*, 962–976. https://doi.org/10.1111/faf.12391.

Stillman, R. A., Railsback, S. F., Giske, J., Berger, U., & Grimm, V. (2015). Making predictions in a changing world: the benefits of individual-based ecology. *BioScience*, *65*, 140–150. https://doi.org/10.1093/biosci/biu192.

Swain, D. P. (2011). Life-history evolution and elevated natural mortality in a population of Atlantic cod (*Gadus morhua*). *Evolutionary Applications*, *4*, 18–29. https://doi.org/10.1111/j.1752-4571.2010.00128.x.

Tesfaye, M., & Getahun, A. (2021). Review on fish stock assessments models with more emphasis on the use of empirical and analytical models for potential yield prediction. *Acta Entomology and Zoology*, *2*, 23–30. https://doi.org/10.33545/27080013.2021.v2.i2a.40.

Uusi-Heikkilä, S. (2020). Implications of size-selective fisheries on sexual selection. *Evolutionary Applications*, *13*, 1487–1500. https://doi.org/10.1111/eva.12988.

Véron, M., Duhamel, E., Bertignac, M., Pawlowski, L., Huret, M., & Baulier, L. (2020). Determinism of temporal variability in size at maturation of sardine *Sardina pilchardus* in the Bay of Biscay. *Frontiers in Marine Science*, *7*, 567841. https://doi.org/10.3389/fmars.2020.567841.

Ward, A. J., Webster, M. M., & Hart, P. J. (2006). Intraspecific food competition in fishes. *Fish and Fisheries*, *7*, 231–261. https://doi.org/10.1111/j.1467-2979.2006.00224.x.

Whitehead, P. J. (1985). FAO species catalogue. Vol. 7: Clupeoid fishes of the world (suborder Clupeoidei). An annotated and illustrated catalogue of the herrings, sardines, pilchards, sprats, shads, anchovies and wolf-herrings. Part 1 - Chirocentridae, Clupeidae and Pristigasteridae. *FAO Fisheries Synopsis (125), Vol. 7, Pt. 1:* 303p. Rome: Food and Agriculture Organization of the United Nations.

Wilensky, U. (1999). NetLogo (and NetLogo user manual). Center for connected learning and computer-based modeling, Northwestern University. http://ccl.northwestern.edu/netlogo.

Supplementary Information

Article: Haberle, I., Bavčević, L., & Klanjscek, T. (2023). Fish condition as an indicator of stock status: Insights from condition index in a food-limiting environment. *Fish and Fisheries*, 00, 1-15. https://doi.org/10.1111/faf.12744.

Data Availability: The data and code underlying the findings of this study are openly available in Zenodo, https://doi.org/10.5281/zenodo.7569367.

S1 DEB-IBM model for gilthead seabream (*Sparus aurata*)

The composite Dynamic Energy Budget - Individual-based model (DEB-IBM) approach was validated on a biologically and ecologically contrasting fish species, artisanally fished and widely aquacultured demersal predator, gilthead seabream (*Sparus aurata*, Sparidae).

S1.1 Biology, ecology and economical importance of *S. aurata*

Gilthead seabream is an euryhaline opportunistic predator common in the Mediterranean Sea, and along the Eastern Atlantic coasts from Great Britain to Senegal, with rare occurrences in the Black Sea (GBIF Secretariat, 2021). It reaches the maximal age of 11 years and total length of 70 cm (common 35 cm), weighting up to 17.2 kg (Froese & Pauly, 2022a). The species dwells on seagrass beds and sandy bottoms, solitary or in small schools, commonly down to 30 m, with adults occasionally diving up to 150 m. It migrates between coastal lagoons and estuaries for feeding during warmer season, and open water for breeding during winter (Crosetti et al., 2014). Gilthead seabream is a protandrous hermaphrodite, maturing as a male at the age of about 2 years, and starting to reproduce as a female after reaching the size of 30 cm, generally in the second spawning season. The sequenced spawning occurs throughout 3 months in late autumn and winter season.

The gilthead seabream is mostly aquacultured species, however total production from capture fisheries also remains stable in recent years, adding up to 8,646 tonnes/year in 2020 (FAO, 2022). Although this represents only about 3% of the total production (290,720 tonnes in 2020), wild gilthead fisheries still remains an important practice securing social, economic, and nutritional well-being of small local communities (Jentoft et al., 2017; Smith & Basurto, 2019).

S1.2 Modelling procedure

We applied the same modelling approach as described in the Methods section of the main text and in the ODD protocol (Supplement S2). The environmental factors, temperature and total food availability, were fixed to 20°C, and 70 and 3500 $^{J}/_{l}$ for low and high environmental carrying capacity scenario, respectively.

Re-parameterisation The initial DEB parameter set of gilthead seabream was taken from the Add-my-Pet collection entry (Lika & Kooijman, 2016), however the realism of model performance did not prove satisfactory. Because the initial AmP parameter set was parameterized using larvae growth data only, it has under-performed when simulating the whole life cycle, especially underestimating the maximal condition index of adults. We therefore re-parameterized the species with additional dataset on adult growth at *ad-libitum* feeding, taken from Bavčević et al. (2010) - a control group from a starvation experiment. The parameterization followed the AmP estimation procedure using the DEBtool software (DEBtool, 2022; Lika et al., 2011; Marques et al., 2018). The newly obtained parameter set (Table S1.1) was tested for performance, which was satisfactory, and was further used in simulations.

Hermaphroditism To address the protandrous hermaphroditism of gilthead seabream, all juveniles were assigned males at birth, and a sex change algorithm - executed within the *Aging* submodel - was included. The algorithm was run for an individual when specific conditions were met: (i) the individual was more than 2 years old, and (ii) it spawned as a male at least once. The probability of changing sex was set to 0.2 (Liarte et al., 2007) and was lowered to 0.005 when the $^{M}/_{F}$ sex ratio was below 1.18 (Hadj-Taieb et al., 2013).

Table S1.1: DEB-IBM parameters for gilthead seabream (*Sparus aurata*, Sparidae). The dots above the letters denote rates, while square and curly brackets relate to volume- and surface-specific quantities, respectively.

Primary DEB parameters	**Symbol**	**Value**	**Unit**
Maximal surface-specific searching rate†	$\{\dot{F}_m\}$	6.5	$^{l}/_{d\ cm^2}$
Maximum surface-specific assimilation rate	$\{\dot{p}_{Am}\}$	18.5661	$^{J}/_{d\ cm^2}$
Fraction of food energy fixed in reserve†	κ_X	0.80	–
Allocation fraction to soma	κ	0.9409	–
Fraction of reproduction energy fixed in eggs	κ_R	0.95	–
Energy conductance	$\dot{v}$	0.0387	$^{cm}/_{d}$
Volume-specific somatic maintenance rate	$[\dot{p}_M]$	14.49	$^{J}/_{d\ cm^3}$
Volume specific costs of structure	$[E_G]$	5236	$^{J}/_{cm^3}$
Maturity maintenance rate coefficient	$\dot{k}_J$	0.002	$/_{d}$
Maturation threshold for birth	E_H^b	0.0488	J
Maturation threshold for metamorphosis	E_H^j	380.6	J
Maturation threshold for sexual maturation	E_H^p	191400	J

†Used to calculate half-saturation constant K_X

Auxiliary DEB parameters	**Symbol**	**Value**	**Unit**
Half-saturation constant‡	K_X	70	$^{J}/_{l}$
Shape coefficient (larvae)	δ_{Ml}	0.1414	-
Shape coefficient (adult)	δ_{Ma}	0.2422	-
Specific structure density	d_V	0.2	$^{g}/_{cm^3}$
Mass-energy-weight couplers	ω_E	23.9	$^{g}/_{mol}$
	μ_E	550000	$^{J}/_{mol}$
Wet/dry weight coefficient	w	5	-
Acceleration factor§	s_M	$min(\frac{L}{L_b}, \frac{L_j}{L_b})$	-
Inital energy reserve of an egg ¶	E_0	$\frac{E_{0max}-E_{0min}}{[E_m]-[E_{pmin}]}\big([E]-[E_{pmin}]\big)+E_{0min}$	J

‡ Calculated as $\frac{\{\dot{p}_{Am}\}s_M}{\kappa_X\{\dot{F}_m\}}$ and rounded to the nearest 5.

§ Acceleration factor changes with size up to metamorphosis, and is calculated as a ratio of current size L, to the size at birth L_b, $\frac{L}{L_b}$. It stays equal to $\frac{L_j}{L_b}$ after metamorphosis, where L_j is size at metamorphosis.

¶ Determined according to maternal effect, i.e. depends on the actual energy density of the mother $[E]$. $[E_m]$ and $[E_{pmin}]$ are the maximal and minimal energy densities of a fertile mother producing viable eggs with respectively maximal, E_{0max}, and minimal, E_{0min}, initial energy content.

Mortality parameters	**Symbol**	**Value**	**Unit**
Eggs	M_{egg}	0.9996	%
Juveniles	$\dot{M}_j$	1.19‖	$/_{y}$
Adults	$\dot{M}_a$	0.34††	$/_{y}$
Fishing	$\dot{M}_f$	range from 0 to 4	$/_{y}$

‖ Mortality calculated from survival until recruitment reported for white seabream (Cuadros et al., 2018)

†† Average mortality rate reported in the literature (Akyol & Gamsiz, 2011; Kraljević & Dulčić, 1997)

S1.3 Results

The DEB-IBM model successfully simulates population dynamics as well as individual life history traits of gilthead seabream (*Sparus aurata*), validating our modelling approach. The pattern of how fishing mortality and environmental carrying capacity affect individual and population traits (Figures S1.2 and S1.3) is equivalent to the patterns observed for European pilchard (*Sardina pilchardus*). Condition index, weight, and length are positively correlated with increase of fishing mortality, while age at sexual maturation is negatively correlated, for both carrying capacity scenarios (Figure S1.2 a, c and e). Both stock abundance and biomass decrease as the fishing mortality increases (Figure S1.2 b and d). Fished biomass increases up to a fishing mortality of 2.6 per year for both carrying capacity scenarios (Figure S1.2f).

Gilthead seabream is more susceptible to higher fishing mortalities, and experiences population collapse at fishing mortalities above 2.8 and 3 per year for low and high carrying capacity scenario, respectively. This arises from the fact it has a slower life cycle, and needs the double the time to mature compared to the sardine, resulting in slower recruitment.

Correlation between individual traits and abundance shows the same pattern in both carrying capacity scenarios (Figure S1.3), and is equivalent to the one observed for European pilchard. The average functional response, condition index, and weight are inversely correlated with the stock size, while age at sexual maturation increases as the stock size increases.

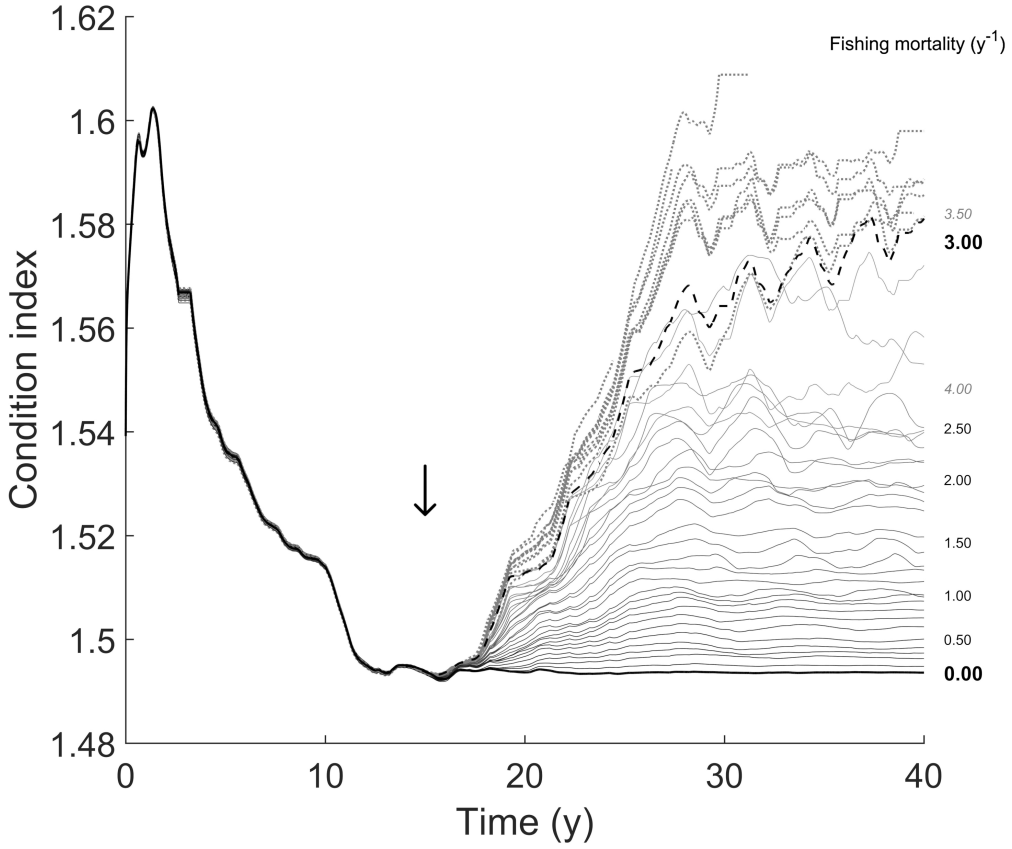

Figure S1.1: Condition index of gilthead seabream (*Sparus aurata*) at different fishing mortalities for high carrying capacity scenario. The records correspond to a 10-year average condition index of adult females. Thick solid line represents the non-fished population, dashed line corresponds to F_{ms}, i.e. maximal fishing mortality that does not lead to a population collapse (3 per year). Dotted lines are simulations at fishing mortality rates $\geq$3.1 per year, resulting in population collapse. The arrow indicates introduction of fishing mortality at the end of year 15 of the simulation. Labels on the right represent instantaneous fishing mortality rates corresponding to the respective lines; note that only every 5^{th} simulation is labeled, and fishing mortailites causing population collapse are indicated in italic.

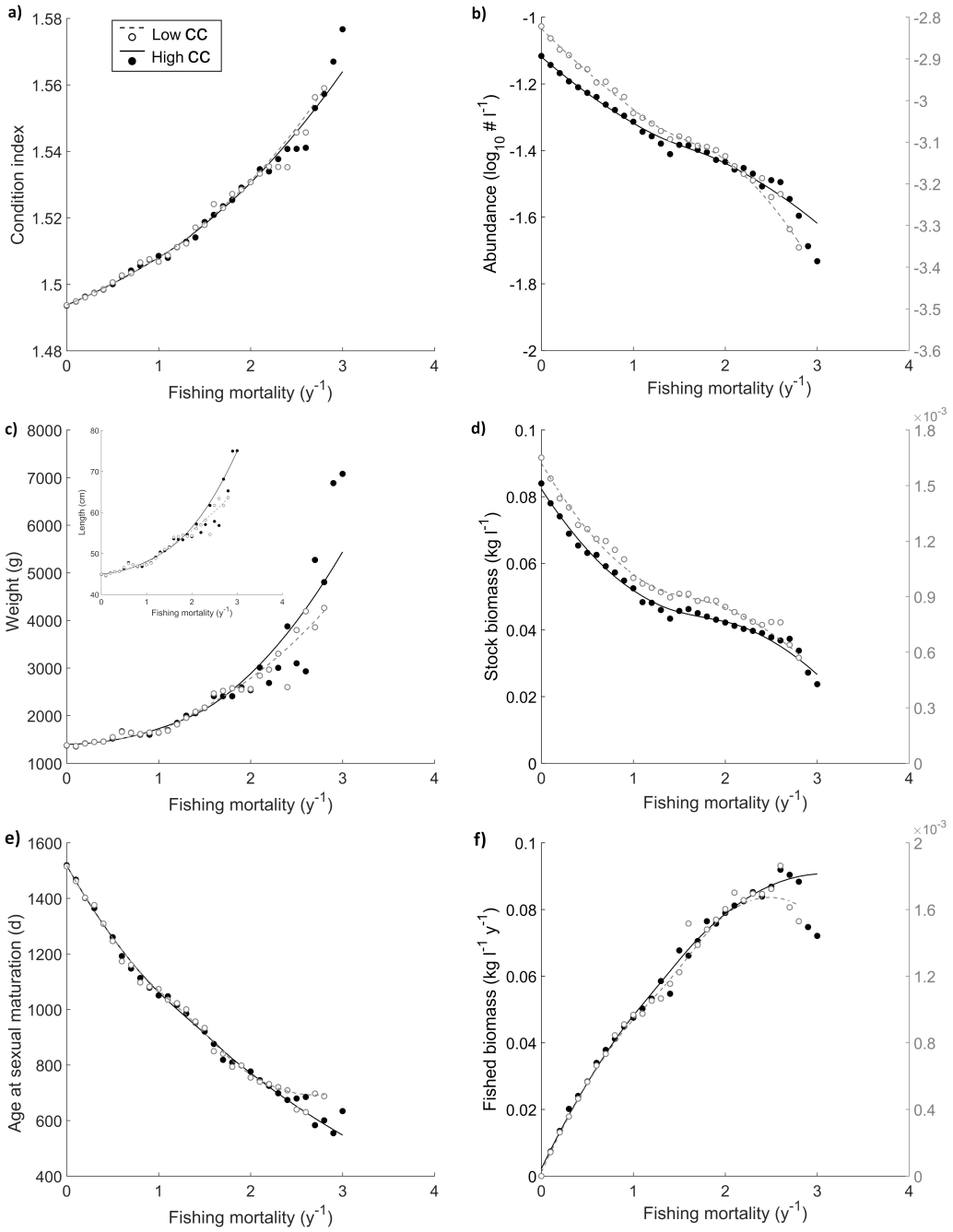

Figure S1.2: Impact of fishing mortality on individual-level (left panels) and population-level (right panels) traits of adult gilthead seabream (*Sparus aurata*), for high and low environmental carrying capacities. Markers represent a 10-year average recorded at the end of each simulation, and the lines are moving average regressions; only simulations up to F_{ms}, 2.8 and 3 per year for high and low carrying capacity, respectively, are shown. Right y-axes on panels (b), (d), and (f) correspond to the low carrying capacity scenario. Individual condition index (a), weight (c), and length (c - insert) increase, and the time to reach sexual maturation (e) decreases with fishing mortality, for both carrying capacity scenarios. Stock size (b) and biomass (d) decrease with fishing mortality for both scenarios. Fished biomass (f) increases up to a fishing mortality of 2.3 per year for low, and 2.4 per year for high carrying capacity scenario, and decreases afterwards. Note fishing mortality is expressed as instantaneous fishing mortality rate per year. Also note the log_{10} scale is used for the visualization of abundance in panel (b).

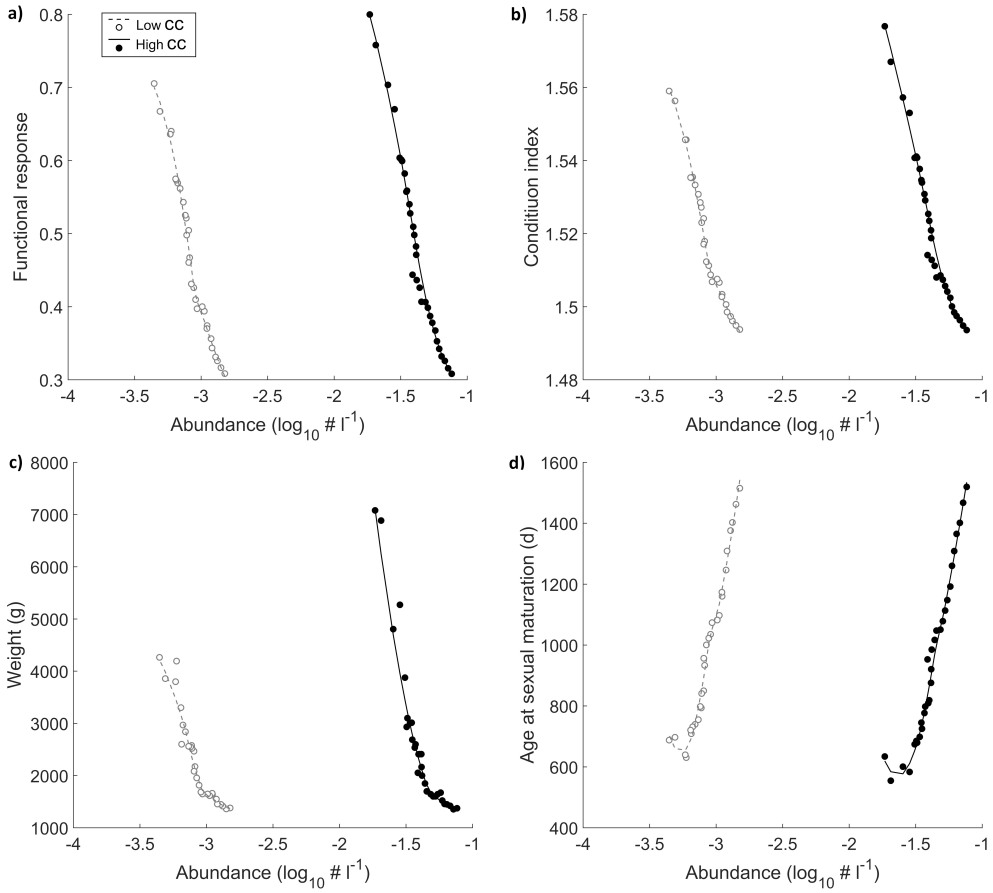

Figure S1.3: Functional response and individual-level traits of adult gilthead seabream (*Sparus aurata*) at a steady state, for low and high carrying capacity scenarios, as functions of adult fish abundance (stock size). Markers represent a 10-year average recorded at the end of each simulation, and the lines are moving average regressions; only simulations up to F_{ms}, 2.8 and 3 per year for high and low carrying capacity, respectively, are shown. Functional response (a), condition index (b), and weight (c) decrease, while age at sexual maturation (d) increases with abundance for both carrying capacity scenarios. Note the abundance (x-axis) is log_{10} transformed for easier visualization.

S2 ODD (Overview, Design concepts, and Details) protocol

S2.1 Purpose

The purpose of the composite model is to correlate the individual-level processes and population-level responses, creating a link between physiological state of the individual to the status of its population. The state of the individual is simulated using the Dynamic Energy Budget (DEB) model, and is then correlated to the population traits through the integration with the individual-based model (IBM).

S2.2 Entities, state variables, and scales

The two main components in the model are individuals and their environment.

Individuals There are three types of individuals based on their developmental status: EggMasses, Juveniles and Adults. Each individual is characterised by four standard DEB state variables: (i) structure, determining the actual size, and governing feeding and maintenance, (ii) energy reserve, serving as an intermediate energy storage between energy uptake and its mobilization, (iii) maturity, determining the transitions between the developmental stages at fixed maturity levels, and (iv) reproduction buffer, filled with energy only in the Adult individuals, allowing for production of offspring.

Environment Environment is defined with two factors: temperature and food availability (determining the food-limited environmental carrying capacity).

Temperature is a fixed parameter, and kept constant at 20°C in all simulations.

Food is the only forcing variable in our model. Food amount emerges from a concept of constant and food-limited environmental carrying capacity for the species of interest. In such a system, the total daily available food for the whole population is constant, and therefore determines the carrying capacity. We simulate two environmental carrying capacity scenarios, high and low. Within each scenario, the total amount of food available to the whole population at each time-step, X, is constant, and determines the communal functional response of the population, f_{comm}, according to the number of individuals and their size. For the low carrying capacity scenario, X is set to be close to the half-saturation constant of the species, as defined by the DEB parameters ($X \approx K_X$, rounded down to

the nearest 10). For the high carrying capacity scenario, X is set to be 50 times higher. The X value is further used as an input for the *Food update* submodel as described in the section S2.7.

There is no spatial dimension in the model, and the time is continuous, allowing for use of ordinary differential equations.

S2.3 Process overview and scheduling

The individual's DEB state variables are updated based on the set of differential equations calculated in the *DEB* submodel (Section S2.7; Table S2.1). Individuals assimilate energy from the environment into the energy reserve, and mobilise it to the processes of growth, maintenance, and maturation or reproduction. If the individual lacks energy to pay somatic maintenance costs from its reserve, the Juveniles will die immediately, however the starvation mode will be activated for Adults, with reproduction buffer serving as an energy source. For the Juveniles, if maturity reaches sexual maturation threshold, the individual will become an Adult, it will stop investing energy into maturation, and will start to fill its reproduction buffer. During the spawning period, defined by the user, adult Females will produce one EggMass daily, each containing batch of potential offspring. Each EggMass follows its own energy budget dynamics. Once maturity threshold for birth is reached, EggMasses are subject to a mortality event that immediately eliminates a fraction of eggs (M_{egg}) they are holding - this fraction corresponds to the eggs assumed to die within first few days pre-/post-hatch due to natural mortality. Surviving eggs hatch into Juveniles.

After initial setup of the model, when the environment is defined and the desired number of individuals is created, the algorithm at each time-step is as follows:

- Check timing
  - Apply fishing mortality after 15 years of simulation
  - Terminate the simulation if (i) timing $\geq$40 years and steady state criteria is reached, or (ii) all individuals are dead, i.e. population is extinct.
    Steady state criteria: a 2-year average value of f_{comm} coincides with the 10-year average, i.e. the two averages do not differ more than $\pm$ 1%

- Update environment - calculate communal functional response, f_{comm}, corresponding to the food availability and the population size
- Determine survival of each individual according to natural and fishing mortality ($\dot{M}_j$, $\dot{M}_a$, $\dot{M}_f$)
- Update DEB of each individual
  - Calculate energy fluxes: $\dot{p}_A$, $\dot{p}_C$, $\dot{p}_S$, $\dot{p}_J$, $\dot{p}_G$, $\dot{p}_R$
  - Calculate change of energy reserve
  - Calculate change of structure
  - If not mature: calculate change of maturity
  - If mature: calculate change of reproduction buffer
  - If mobilisation to soma $<$ somatic maintenance: Juveniles die, Adults use starvation mode or die if no energy is available
- Hatch Juveniles from EggMasses that reached maturity for birth
- Matamorphose/mature Juveniles
  - Metamorphose all Juveniles that reached maturity threshold for metamorphosis
  - Mature all Juveniles that reached sexual maturation threshold into Adults
- Spawn
  - Females create EggMass investing a fraction of reproduction buffer energy
  - Males spend same amount of energy for fertilization
- Increase age of each individual
- If hermaphroditism applies, change sex of the individuals that meet the conditions
- Update simulation timing
- Record data

S2.4 Design concepts

Basic principles The model is built upon principles of both DEB theory and IBMs. The DEB sets a mass-energy balance theoretical framework for governing metabolic processes of the individual, and allows for description of assimilation and utilization of energy for growth, maintenance and reproduction. IBM framework enables translation of individual dynamics to the population level.

Emergence All individual traits (length, weight, energy reserve, reproduction output), and arising population trends (abundance, biomass), emerge from the properties of metabolic organization introduced by the DEB theory, as well as through inter-individual interactions and individuals' interaction with the environment.

Adaptation and objectives Largest individuals have priority in mating, where dominant (larger) females are first to be paired with available mates, followed by subordinate (smaller) females, until there are enough males available to fertilize the eggs (1 male can mate with up to 10 females).

Learning, prediction, sensing Individuals do not learn or express cognition, nor they predict future conditions. They sense their environment through temperature and food availability. If hermaphroditism applies (such as for gilthead seabream), males sense the abundance of females during sex change process, which corresponds to sensing of pheromones (Devlin & Nagahama, 2002). The probability of changing sex from male to female decreases if the sex ratio is below common value expected in the wild (e.g. $^{M}/_{F} = 1.18$ for gilthead seabream; Hadj-Taieb et al. 2013).

Interaction Individuals interact indirectly through food competition, with the communal functional response decreasing as the abundance and the size of the individuals increase. Another interaction is during the spawning season, with females pairing with available males to reproduce.

Stochasticity The order in which the individuals are processed each time-step is stochastic, as per default setting in NetLogo that selects individuals in a random order. The definition of the initial population is also stochastic, with the size of the individuals randomly

drawn from a normal distribution using the built-in NetLogo *random-normal* function, and within a range defined by the *bound* function. Individual survival and (if applicable) sex change are also stochastic, complying with calculated probabilities. We use the built-in *random-float 1* function to randomly draw a number between 0 and 1, which is then compared to the calculated probability - if the randomly drawn number is equal or lower, the event (death, sex change) occurs.

Collectives Individuals belong to a specific group according to their maturity (Juveniles, Adults) and sex (Males, Females), which define their participation in the breeding process - Juveniles do not mate, while Adults do, with only Females creating EggMasses.

Observation At each time-step the model tracks (i) population trend through fish density and stock biomass, and (ii) average individual traits for Juveniles and adult Females, including functional response, length, weight, condition index, energy reserve, time at sexual maturation (Juveniles only), and energy invested into reproduction (adult Females only). NetLogo interface allows for direct monitoring of single values, along with a real-time graphical visualization of resulting time-series. A set of simulations for each scenario is pre-setup and run through the NetLogo BehaviorSpace tool, and both individual and population traits are simultaneously recorded into an extensive .csv file (as described in Wilensky, 1999), allowing for later analysis.

S2.5 Initialization

The model initialization consists of setting up the DEB and IBM parameters, the environment, and the initial population. Initial DEB parameters were taken from the AmP (2023) and a test simulation was run to inspect their performance. Preliminary simulations for European pilchard yielded realistic outcomes, so the initial parameters were kept 'as-is' in further simulations (Table 1). Preliminary simulations for gilthead seabream, however, did not prove satisfactory, and a new parameter set was obtained as described in Supplement S1.2. The temperature was constant 20°C for both species, and the amount of total available food was set according to the carrying capacity scenario, to the value determined as previously described (Section S2.2). The initial population size was set to be close to the equilibrium value of the non-fished population, and consisted of adults only, with male to female sex-ratio within the reported range (0.88 - 1.28 for European pilchard, Keznine

et al. 2020; Mustač & Sinovčić 2010; 1.18 - 1.28 for gilthead seabream, Hadj-Taieb et al. 2013; Kraljević 2009). The initial size of each individual was randomly assigned from a normal distribution with the mean corresponding to the common length (20 cm for European pilchard; 35 cm for gilthead seabream; Froese & Pauly 2022b) and a standard deviation 5 cm. The age was defined according to the scaled length ($^{\text{length}}/_{\text{maximal length}}$). Weight, structure, and reserve were derived from the assigned size using equations for conversion between empirical and abstract DEB variables (Table S2.1), and assuming functional response $f = 0.8$. Maturity was set to maturity at sexual maturation, and reproduction buffer was empty. For gilthead seabream spawning indicator for all males was set to 0, preventing their sex change before their first reproduction.
The volume of the modeled basin was selected according to the modelling requirements for each scenario and species, small enough to reduce the computing time, and large enough to avoid stochastic extinction of the initial population.

S2.6 Input data

Currently, there are no data inputs from external files, however this can be easily included in the future to accommodate for time-varying variables, such as fluctuating temperature.

S2.7 Submodels

Time management The time-track section is incorporated within the main section of the model and is designated to (i) apply fishing mortality, (ii) call for *Spawning* submodel, and (iii) terminate simulation, at defined conditions.

Food update Food is updated each time-step as a total daily available food, expressed as a concentration of energy X ($^{\text{J}}/_{\text{l}}$). The value was pre-determined as described in the Section S2.2 and kept constant throughout the simulation. At each time-step the total available food is equally distributed amongst all individuals based on the collective assimilation dictated by the DEB model. A communal functional response of all individuals, f_{comm}, is calculated as a ratio of the total food assimilation of the population ($\dot{p}_A$) to the maximal possible assimilation of the population ($\dot{p}_{Amax}$).

$$f_{comm} = min\left(\frac{\dot{p}_A}{\dot{p}_{Amax}}, 1\right) \tag{S2.1}$$

Assuming all available food can potentially be consumed by the population, the total food assimilation of the population equals the assimilation of all available food X in the system volume W_V, with the energy fixation efficiency κ_X, within the model time-step Δt,

$$\dot{p}_A = \frac{\kappa_X X W_V}{\Delta t}. \tag{S2.2}$$

The maximal possible assimilation of the population ($\dot{p}_{Amax}$) equals to the sum of individual maximal assimilation ($\dot{p}_{Amax_i}$, i indicating individual) of its N individuals, determined by their size L_i,

$$\dot{p}_{Amax} = \sum_{i=1}^{N} \dot{p}_{Amax_i} = \sum_{i=1}^{N} \left\{\dot{p}_{Am}\right\} s_{M_i} L_i^2. \tag{S2.3}$$

Integrating Eq. S2.2 and S2.3 into Eq. S2.1 we obtain the communal functional response

$$f_{comm} = min\left(\frac{\kappa_X X W_V}{\Delta t \sum_{i=1}^{N} \left\{\dot{p}_{Am}\right\} s_{M_i} L_i^2}, 1\right) \tag{S2.4}$$

that is further used to calculate actual individual assimilation as described below in the *DEB* submodel.

Survival The *Survival* submodel distinguishes between Juveniles that die due to the natural mortality only, and Adults that are also affected by the fishing mortality. Death of each individual is a stochastic event with the mortality probability calculated as

$$M = 1 - e^{-(\dot{M}_n + \dot{M}_f)\Delta t} \tag{S2.5}$$

where $\dot{M}_n$ is a natural mortality rate, different for each life stage, and $\dot{M}_f$ is the instantaneous fishing mortality rate applied only to Adults, otherwise being 0. The model tracks the amount of fish being caught, i.e. counts the fish that died exclusively due to fishing, and would survive otherwise.

Dynamic Energy Budget The DEB model is run separately for each individual, calculating energy fluxes and emerging energy dynamics dictating growth, development and reproduction.

Individual assimilation is determined by the communal functional response, f_{comm},

calculated in the *Food-update* submodel, and by the size of the individual L_i

$$\dot{p}_{A_i} = f_{comm}\{\dot{p}_{Am}\} s_{M_i} L_i^2. \tag{S2.6}$$

Mobilisation depends on current energy reserve and the size of the individual

$$\dot{p}_C = \frac{E}{V} \cdot \frac{\dot{v} s_{M_i} [E_G] V^{2/3} + \dot{p}_S}{\kappa^E/_V + [E_G]} \tag{S2.7}$$

where $V = L_i^3$, and with $\dot{p}_S$ being somatic maintenance

$$\dot{p}_S = [\dot{p}_M] V. \tag{S2.8}$$

Change in energy reserve is calculated as a difference between assimilated and mobilised energy

$$dE = \dot{p}_{A_i} - \dot{p}_C. \tag{S2.9}$$

A fraction of mobilized energy, $\kappa \dot{p}_C$, goes to the somatic branch where it first pays somatic maintenance, with the remaining energy supporting growth of the organism, i.e. change in structure

$$dV = \frac{\dot{p}_G}{[E_G]} = \frac{\kappa \dot{p}_C - \dot{p}_S}{[E_G]}. \tag{S2.10}$$

The model performs an internal check whether there is enough energy to pay somatic maintenance costs from its energy reserve. If this is not true, the Juveniles will die immediately, and starvation mode will be activated for Adults. Starvation mode allows reallocation of energy from the reproduction buffer to pay somatic maintenance.

The other fraction of mobilized energy, $(1 - \kappa)\dot{p}_C$, goes to the reproductive branch, first paying maturity maintenance, and the rest being allocated to maturity or reproduction. Maturity tracks individual development and it will increase until sexual maturation, remaining constant afterwards. After sexual maturation, energy is allocated into the reproduction buffer. The flux of energy into maturation/reproduction is described as

$$\dot{p}_R = (1 - \kappa)\dot{p}_C - \dot{p}_J \tag{S2.11}$$

with $\dot{p}_J$ being maturity maintenance

$$\dot{p}_J = \dot{k}_J E_H. \tag{S2.12}$$

Consequentially, dynamics of maturity and reproduction buffer is

$$dE_H \veebar dE_R = \dot{p}_R. \tag{S2.13}$$

All DEB state variables are updated, and translated into biological metrics - physical length and weight

$$L_w = \frac{V^{1/3}}{\delta_M}, \tag{S2.14}$$

$$W_w = \mathrm{w}\left(d_V V + \frac{\omega_E}{\mu_E}(E+R)\right). \tag{S2.15}$$

Ultimately, Fulton's condition index (K) is calculated as a ratio of physical weight (g) to cubed length (cm^3) (Ricker, 1975), and scaled by a factor 100 to bring the value close to unity

$$K = 100\frac{W_w}{L_w^3}. \tag{S2.16}$$

The DEB of EggMasses is calculated in the same way as described above, except they do not feed, thus their assimilation equals 0.

Hatching Each EggMass that has reached maturity threshold for birth will release a certain number of offspring, defined by the amount of energy allocated to the EggMass at spawning (see *Spawning* submodel below). A one-time mortality event is applied immediately at hatching, killing off a fraction of the total number of offspring, according to the egg mortality, M_{egg}. Survived larvae keep the structure (size), energy reserve, and maturity of the egg they are hatched from, and their reproduction buffer is set to 0.

Maturation Each Juvenile metamorphoses from larvae to adult-looking fish once maturity threshold for metamorphosis is reached. This is reflected in the value of acceleration factor, s_M, affecting assimilation and mobilisation. Acceleration factor changes with size up to metamorphosis, and is calculated as a ratio of current size L, to the size at birth L_b: $\frac{L}{L_b}$. It stays constant after the metamorphosis, equal to $\frac{L_j}{L_b}$, where L_j is the size at metamorphosis. Once maturity threshold for sexual maturation is reached, Juveniles

become Adults, they stop investing energy into maturation, and start to reproduce.

Spawning *Spawning* submodel transfers energy contained in the reproduction buffer of Adults into gametes. Each Female needs to be paired with a Male to be able to produce fertile eggs. Each Male can be paired with up to 10 Females. When paired, Female creates one EggMass per time-step, allocating a fraction of total energy contained in the reproduction buffer according to the reproduction efficiency κ_R, and proportional to the duration of the spawning season. The number of eggs an EggMass will hold is determined by the total energy allocated to the EggMass, and the initial energy reserve of an egg, E_0. The initial energy reserve is calculated according to the maternity effect, i.e. depending on the energy reserve density, $[E]$, of the mother

$$E_0 = \frac{E_{0max} - E_{0min}}{[E_m] - [E_{pmin}]}\big([E] - [E_{pmin}]\big) + E_{0min} \tag{S2.17}$$

where $[E_m]$ and $[E_{pmin}]$ are the maximal and minimal energy densities of a fertile mother, producing viable eggs with respectively maximal, E_{0max}, and minimal, E_{0min}, initial energy reserve.

Males spawning is addressed in a similar way, deducing a corresponding fraction of energy from their reproduction buffer each time-step during spawning season, however without creation of EggMasses.

Aging Within *Aging* submodel the age of each individual is increased by 1 day each time-step. If hermaphroditism applies, additional algorithm for sex change is run once the conditions are met, with the probability of sex change calculated according to the reported values.

Table S2.1: Summary of primary equations used in the composite DEB-IBM model. Parameters are as defined in the Tables 1 and S1.1. The symbols for the DEB state variables are as used in the NetLogo model code: En - energy reserve, V - structure, H - maturity, R - reproduction buffer.

Environmental forcing	
Food[†]	$f_{comm} = min\left(\frac{\kappa_X X W_V}{\Delta t \sum_{i=1}^{N}\left\{\dot{p}_{Am}\right\} s_{M_i} L_i^2}, 1\right)$

[†] Food defines a communal functional response, f_{comm}, according to the total daily available food X ($^{J}/_{l}$) in the system volume W_V, and the maximal possible assimilation of the population, i.e. the sum of individual maximal assimilation of all its N individuals.

DEB energy flux	
Assimilation[‡]	$\dot{p}_{A_i} = f_{comm}\left\{\dot{p}_{Am}\right\} s_{M_i} L_i^2$
Mobilization[§]	$\dot{p}_C = [E] \cdot \frac{\dot{v} s_{M_i} [E_G] V^{2/3} + \dot{p}_S}{\kappa [E] + [E_G]}$
Somatic maintenance	$\dot{p}_S = [\dot{p}_M] V$
Maturity maintenance	$\dot{p}_J = \dot{k}_J H$
Growth	$\dot{p}_G = \kappa \dot{p}_C - \dot{p}_S$
Maturation/Reproduction	$\dot{p}_R = (1-\kappa)\dot{p}_C - \dot{p}_J$

[‡] Assimilation starts at birth, i.e. when $H \geq E_H^b$; it is equal to 0 before birth.

[§] $[E]$ stands for energy density, $^{En}/_{V}$.

Dynamics of the DEB state variables	
Reserve energy	$\frac{d}{dt} En = \dot{p}_{A_i} - \dot{p}_C$
Structural body volume	$\frac{d}{dt} V = \frac{\dot{p}_G}{[E_G]}$
Energy invested into maturation	$\frac{d}{dt} H = \dot{p}_R$ while $H < E_H^p$
Energy invested into reproduction	$\frac{d}{dt} R = \dot{p}_R$ when $H = E_H^p$

Calculation of biological metrics	
Length	$L_w = \frac{V^{1/3}}{\delta_{M_i}}$
Weight	$W_w = \mathrm{w}\big(d_V V + \frac{\omega_E}{\mu_E}(En + R)\big)$
Fertility	$N_{eggs} = \kappa_R \frac{R}{E_0}$
Fulton's condition index	$K = 100 \frac{W_w}{L_w^3}$

Mortality probability	$M = 1 - e^{-(\dot{M}_n + \dot{M}_f)\Delta t}$

S3 Chemostat type food dynamics

To demonstrate that observed patterns of the individual- and population-level traits with fishing mortality hold regardless of the food dynamics, we performed additional simulations where we give food its own dynamic. As opposed to the static food, here we use the chemostat type dynamics described in De Roos et al. (1990), where change in food, ΔX, is calculated as

$$\Delta X = r(X_{max} - X) - I \tag{S3.1}$$

where r represents flow-through rate, X_{max} maximal food in the system (i.e. without predators), X is the current food availability, and I denotes ingestion by predators. The value of X_{max} was selected to allow the environmental carrying capacity for fish that coincided with the one used with static food: $X_{max} \approx 2K_X$ for low, and 50 times higher for high carrying capacity scenario. At each time-step, we first calculated the food production, $r(X_{Max} - X)$, and summed it with the existing food to arrive at the total available food for that time-step, $X = X + r(X_{Max} - X)$. We then followed the same approach as with the static food, determining the communal functional response, f_{comm}, and calculating ingestion of each individual accordingly (for more details, please consult IBM section of the Methods in the main text and the ODD protocol in the Supplement S2). Total consumed food was subtracted from the total available food, and the remaining food was passed to the next time-step.

The observed patterns indicate the robustness of our results: in both carrying capacity scenarios, condition index, weight, and length increase, while age at sexual maturation, stock abundance, and stock biomass decrease with the fishing mortality (Figure S3.1); also, functional response, condition index, and weight are negatively correlated with the stock abundance, while age at sexual maturation shows positive correlation (Figures S3.2).

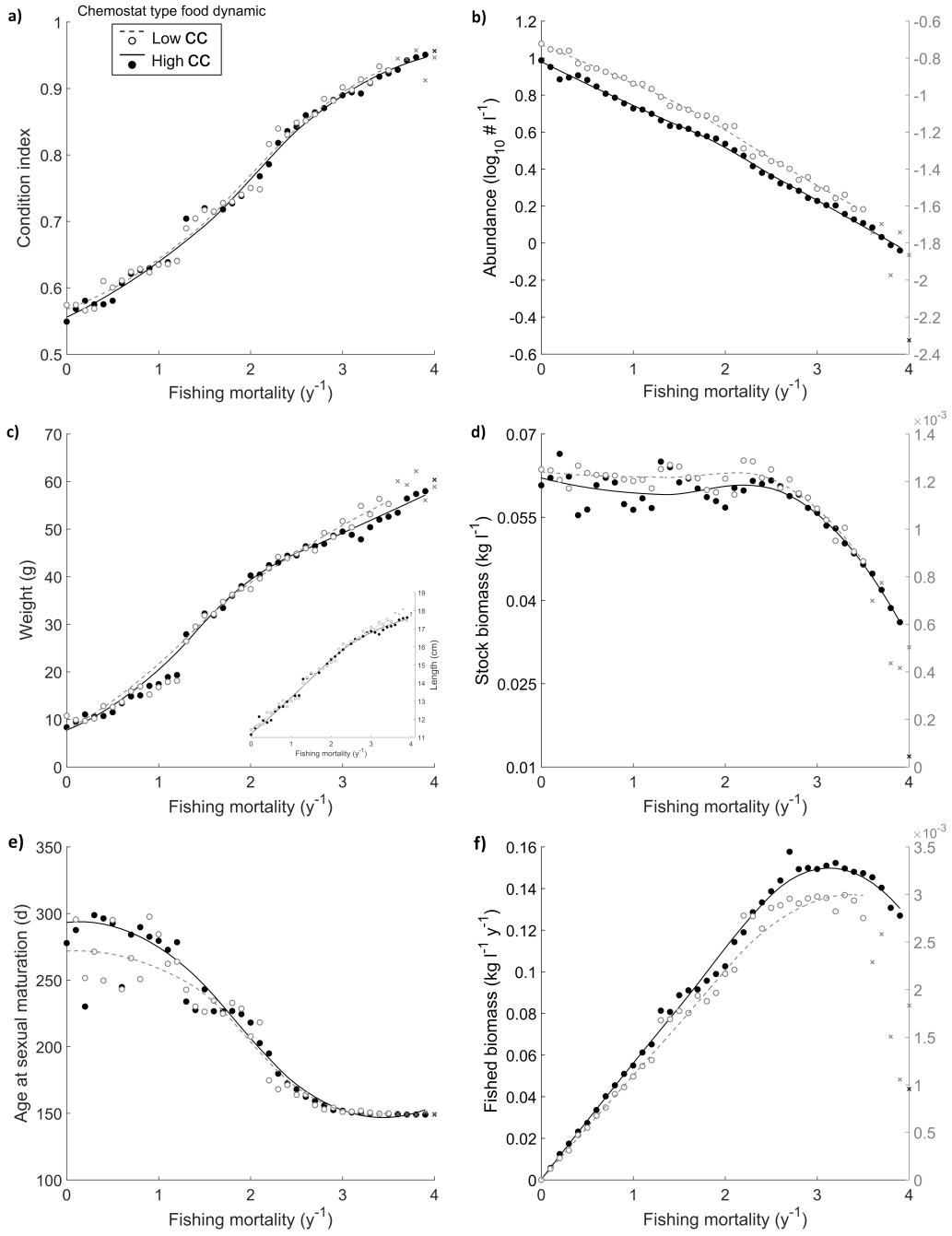

Figure S3.1: Impact of fishing mortality on individual-level (left panels) and population-level (right panels) traits of adult European pilchard (*Sardina pilchardus*), for high and low environmental carrying capacities, with chemostat type food dynamics. Markers represent a 10-year average recorded at the end of each simulation, and the lines are moving average regressions, applied to the non-collapsed populations only (circles); the X markers correspond to the collapsed populations (average population size below 10% of the initial stock size). Right y-axes on panels (b), (d), and (f) correspond to the low carrying capacity scenario. Individual condition index (a), weight (c), and length (c - insert) increase, and the time to reach sexual maturation (e) decreases with fishing mortality, for both carrying capacity scenarios. Stock size (b) decreases with fishing mortality for both scenarios, while stock biomass stagnates up to a fishing mortality of 2.5 per year and decreases thereafter (d). Fished biomass (f) increases up to a fishing mortality of 2.7 per year, and rapidly decreases after 3.4. Note fishing mortality is expressed as instantaneous fishing mortality rate per year. Also note the log_{10} scale is used for the visualization of abundance (b).

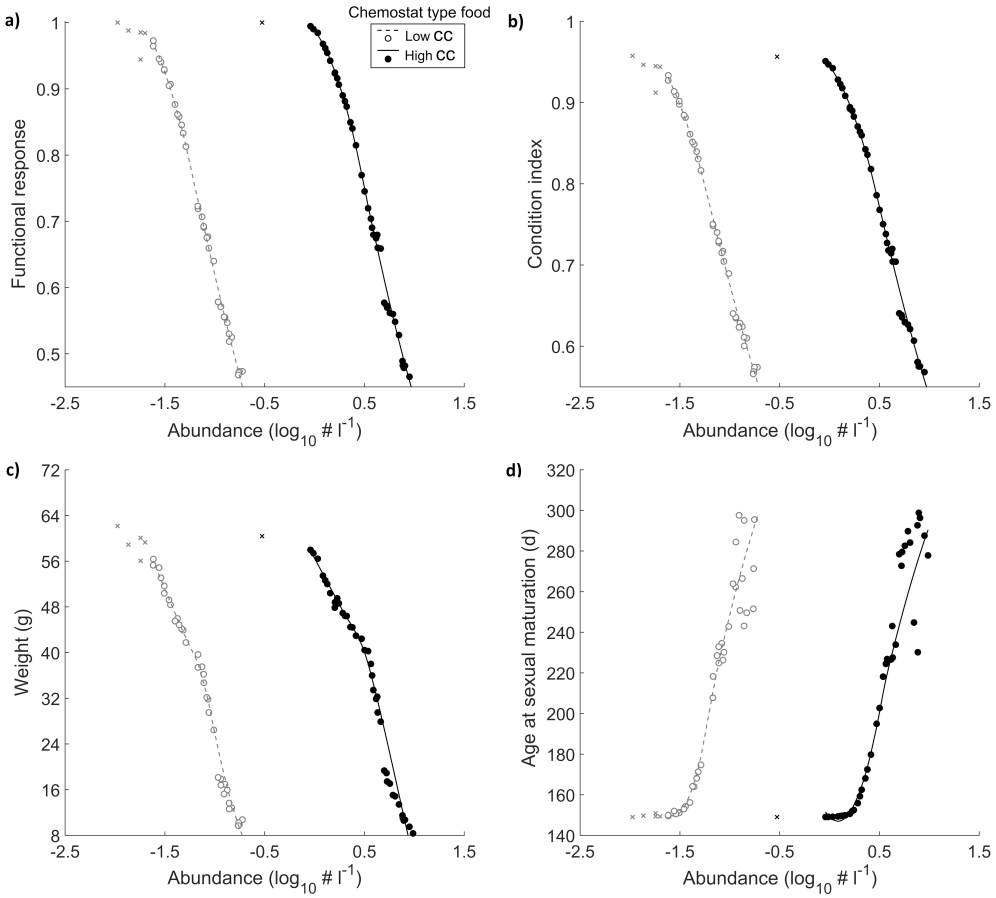

Figure S3.2: Functional response and individual-level traits of adult European pilchard (*Sardina pilchardus*) at a steady state, for low and high carrying capacity scenarios, with chemostat-type food dynamics, as functions of adult fish abundance (stock size). Markers represent a 10-year average recorded at the end of each simulation, and the lines are moving average regressions, applied to the non-collapsed populations only (circles); the X markers correspond to the collapsed populations (average population size below 10% of the initial stock size). Functional response (a), condition index (b), and weight (c) decrease, while age at sexual maturation (d) increases with abundance, for both carrying capacity scenarios. Note the abundance (x-axis) is log_{10} transformed for easier visualization.

References

Akyol, O., & Gamsiz, K. (2011). Age and growth of adult gilthead seabream (*Sparus aurata* L.) in the Aegean Sea. *Journal of the Marine Biological Association of the United Kingdom*, *91*, 1255–1259. https://doi.org/10.1017/S0025315410001220.

AmP (2023). Add-my-Pet collection. https://www.bio.vu.nl/thb/deb/deblab/add_my_pet/species_list.html. Accessed on 30.01.2023.

Bavčević, L., Klanjšček, T., Karamarko, V., Aničić, I., & Legović, T. (2010). Compensatory growth in gilthead sea bream (*Sparus aurata*) compensates weight, but not length. *Aquaculture*, *301*, 57–63. https://doi.org/10.1016/j.aquaculture.2010.01.009.

Crosetti, D., Rossi, A., & De Innocentiis, S. (2014). AquaTrace species leaflet: Gilthead sea bream (*Sparus aurata)*. AquaTrace.

Cuadros, A., Basterretxea, G., Cardona, L., Cheminée, A., Hidalgo, M., & Moranta, J. (2018). Settlement and post-settlement survival rates of the white seabream (*Diplodus sargus*) in the western Mediterranean Sea. *PloS one*, *13*, e0190278. https://doi.org/10.1371/journal.pone.0190278.

De Roos, A., Metz, J., Evers, E., & Leipoldt, A. (1990). A size dependent predator-prey interaction: who pursues whom? *Journal of Mathematical Biology*, *28*, 609–643. https://doi.org/10.1007/BF00160229.

DEBtool (2022). Software package DEBtool_M. https://github.com/add-my-pet/DEBtool_M.

Devlin, R. H., & Nagahama, Y. (2002). Sex determination and sex differentiation in fish: an overview of genetic, physiological, and environmental influences. *Aquaculture*, *208*, 191–364. https://doi.org/10.1016/S0044-8486(02)00057-1.

FAO (2022). Fishery and Aquaculture Statistics. Global production by production source 1950-2020 (FishStatJ). In *FAO Fisheries and Aquaculture Division [online]*. Rome: FAO Fisheries and Aquaculture Department. Updated 2022. FishStatJ software available at: https://www.fao.org/fishery/en/topic/166235.

Froese, R., & Pauly, D. (2022a). Fishbase: *Sparus aurata*. https://www.fishbase.se/summary/Sparus-aurata.html. Accessed on 2.11.2022.

Froese, R., & Pauly, D. (2022b). Fishbase. world wide web electronic publication. www.fishbase.org. Accessed on 2.11.2022.

GBIF Secretariat (2021). GBIF Backbone Taxonomy. https://doi.org/10.15468/39omei. Accessed via https://www.gbif.org/species/2392508 [*Sparus aurata Linnaeus*, 1758] on 03.03.2022.

Hadj-Taieb, A., Ghorbel, M., Hadj-Hamida, N. B., & Jarboui, O. (2013). Sex ratio, reproduction, and growth of the gilthead sea bream, *Sparus aurata* (Pisces: Sparidae), in the Gulf of Gabes, Tunisia. *Ciencias Marinas*, *39*, 101–112. https://doi.org/10.7773/cm.v39i1.2146.

Jentoft, S., Chuenpagdee, R., Barragán-Paladines, M. J., & Franz, N. (2017). *The small-scale fisheries guidelines: global implementation. MARE Publication Series: Volume 14*. Springer International Publishing AG. https://doi.org/10.1007/978-3-319-55074-9.

Keznine, M., Analla, M., Aksissou, M., & El Meraoui, A. (2020). The reproduction and growth of the sardine *Sardina pilchardus* in West Mediterranean, Morocco. *Egyptian Journal of Aquatic Biology and Fisheries*, *24*, 303–319. https://doi.org/10.21608/ejabf.2020.98433.

Kraljević, M. (2009). Some biological and fishery characteristic of Gilthead sea bream, *Sparus aurata* (l.), from the eastern Adriatic Sea. In B. Glamuzina, & J. Dulčić (Eds.), *Ribe i ribarstvo rijeke Neretve: stanje i perspektive* (pp. 127–142). Sveučilište u Dubrovniku i Dubrovačko-Neretvanska Županija.

Kraljević, M., & Dulčić, J. (1997). Age and growth of gilt-head sea bream (*Sparus aurata* l.) in the Mirna Estuary, Northern Adriatic. *Fisheries research*, *31*, 249–255. https://doi.org/10.1016/S0165-7836(97)00016-7.

Liarte, S., Chaves-Pozo, E., García-Alcazar, A., Mulero, V., Meseguer, J., & García-Ayala, A. (2007). Testicular involution prior to sex change in gilthead seabream is characterized by a decrease in DMRT1 gene expression and by massive leukocyte infiltration. *Reproductive Biology and Endocrinology*, *5*, 1–15. https://doi.org/10.1186/1477-7827-5-20.

Lika, D., & Kooijman, B. (2016). AmP *Sparus aurata*, version 2016/10/15. https://www.bio.vu.nl/thb/deb/deblab/add_my_pet/entries_web/Sparus_aurata/Sparus_aurata_res.html. Accessed on 27.10.2022.

Lika, K., Kearney, M. R., Freitas, V., van der Veer, H. W., van der Meer, J., Wijsman, J. W., Pecquerie, L., & Kooijman, S. A. L. M. (2011). The "covariation method" for estimating the parameters of the standard dynamic energy budget model I: Philosophy and approach. *Journal of Sea Research*, *66*, 270–277. https://doi.org/10.1016/j.seares.2011.07.010.

Marques, G. M., Augustine, S., Lika, K., Pecquerie, L., Domingos, T., & Kooijman, S. A. L. M. (2018). The AmP project: Comparing species on the basis of dynamic energy budget parameters. *PLOS Computational Biology*, *14*, 1–23. https://doi.org/10.1371/journal.pcbi.1006100.

Mustač, B., & Sinovčić, G. (2010). Reproduction, length-weight relationship and condition of sardine, *Sardina pilchardus* (Walbaum, 1792), in the eastern Middle Adriatic Sea (Croatia). *Periodicum biologorum*, *112*, 133–138.

Ricker, W. E. (1975). Computation and interpretation of biological statistics of fish populations. *Bulletin of the Fisheries Research Board of Canada*, *191*, 1–382.

Smith, H., & Basurto, X. (2019). Defining small-scale fisheries and examining the role of science in shaping perceptions of who and what counts: A systematic review. *Frontiers in Marine Science*, *6*, 236. https://doi.org/10.3389/fmars.2019.00236.

Wilensky, U. (1999). NetLogo (and NetLogo user manual). Center for connected learning and computer-based modeling, Northwestern University. http://ccl.northwestern.edu/netlogo.